Pontifícia Universidade Católica do Rio Grande do Sul
Faculdade de Biociências
Programa de Pós-Graduação em Biologia Celular e Molecular

Dissertação de Mestrado

Paulo Cesar Patta

Modo de ação da enzima recombinante hipoxantina-guanina fosforribosiltransferase (EC 2.4.2.8) de *Mycobacterium tuberculosis*

Porto Alegre
2014

Paulo Cesar Patta

Modo de ação da enzima recombinante hipoxantina-guanina fosforribosiltransferase (EC 2.4.2.8) de *Mycobacterium tuberculosis*

Dissertação apresentada ao Programa de Pós-Graduação em Biologia Celular e Molecular da PUCRS como requisito para a obtenção do título de Mestre em Biologia Celular e Molecular.

Orientador: Prof. Dr. Luiz Augusto Basso

Porto Alegre
2014

Paulo Cesar Patta

Modo de ação da enzima recombinante hipoxantina-guanina fosforribosiltransferase (EC 2.4.2.8) de *Mycobacterium tuberculosis*

Dissertação apresentada ao Programa de Pós-Graduação em Biologia Celular e Molecular da PUCRS como requisito para a obtenção do título de Mestre em Biologia Celular e Molecular.

BANCA EXAMINADORA:

Prof. Dr. Andre Arigony Souto

Prof. Dr. Osmar Norberto de Souza

Prof. Dr. Mario Sérgio Palma

Porto Alegre
2014

AGRADECIMENTOS

Aos professores Luiz A. Basso e Diógenes S. Santos pela oportunidade de participar do grupo de pesquisas, por possibilitarem o desenvolvimento deste trabalho e pelos ensinamentos que passaram ao longo destes anos.

Aos colegas e ex-colegas do CPBMF pelo apoio na resolução de problemas e no desenvolvimento deste trabalho.

A minha mãe pelo apoio e pelo silêncio nas horas de estudo.

A CAPES pelo apoio financeiro.

"If I only had an hour to chop down a tree, I would spend the first 45 minutes sharpening my axe."

Abraham Lincoln

RESUMO

A Tuberculose (TB) é uma doença infecciosa causada principalmente por *Mycobacterium tuberculosis*. O aumento de pacientes infectados entre a população imunocomprometida e a emergência de cepas resistentes a drogas criam uma necessidade de novas estratégias para tartar a TB. Entender como funcionam as vias metabólicas relevantes, como a via de salvamento de purinas, poderá revelar detalhes do *M. tuberculosis* que poderão ser úteis para o desenvolvimento de novas estratégias de combate a este patógeno. A hipoxantina-guanina fosforribosiltransferase (HGPRT) é uma enzima da familia das purina fosforribosiltransferases (PRTase) e catalisa a conversão de hipoxantina ou guanina e 5-fosforribosilpirofosfato-α-1-pirofosfato (PRPP) em inosina 5'-monofosfato (IMP) ou guanosina 5'-monofosfato (GMP) respectivamente, com a liberação de pirofosfato inorgânico (PPi). Aqui nós descrevemos o modo de ação da HGPRT de *M. tuberculosis* (*Mt*HGPRT) através de análises cinéticas e termodinâmicas. Também foram realizados experimentos para determinar o estado oligomérico da enzima em solução e os efeitos de pH, temperatura e efeitos isotópicos do solvente. Esses dados nos permitem comparar a *Mt*HGPRT com homólogos de outras espécies e procurar por similaridades e diferenças nos seu mecanismo e constantes. Nós esperamos que os experimentos apresentados aqui contribuam para o entendimento da via de salvamento de purinas desse patógeno.

Palavras-chave: HGPRT, Cinética em estado estacionário, Calorimetria de titulação isotérmica.

ABSTRACT

Tuberculosis (TB) is an infectious disease caused mainly by *Mycobacterium tuberculosis*. The increasing number of infected patients among immune compromised populations and emergence of drug-resistant strains has created urgent need of new strategies to treat TB. Understanding relevant pathways (as the purine salvage) will reveal details of *M. tuberculosis* that might be used to develop new strategies to combat this pathogen. Hypoxanthine-guanine phosphoribosyltransferase (HGPRT) is an enzyme from the purine phosphoribosyltransferase (PRTase) family and catalyzes the conversion of hypoxanthine or guanine and 5-phosphoribosyl-α-1-pyrophosphate (PRPP) to inosine 5'-monophosphate (IMP) or guanosine 5'-monophosphate (GMP), and pyrophosphate (PPi). Here we describe the mode of action of *M. tuberculosis* HGPRT (*Mt*HGPRT) through kinetic and thermodynamical analysis. Experiments were also performed to determine the oligomeric state in solution, pH, temperature and solvent isotope effects. These data allows us to compare *Mt*HGPRT to homologues from other species and look for similarities and differences in its mechanism and constants. We hope the experiments presented here will contribute to the understanding of this pathogen purine salvage pathway.

Keywords: HGPRT, PRTases, Steady-State Kinetics, Isothermal Titration Calorimetry.

Lista de Ilustrações

Sumário

CAPÍTULO 1

INTRODUÇÃO E OBJETIVOS

1. Introdução

1.1 A Tuberculose

A tuberculose (TB) é uma doença infectocontagiosa causada pelo agente etiológico *Mycobacterium tuberculosis* (MTB). Outros bacilos do gênero *Mycobacterium*, como o *Mycobacterium bovis* e *o Mycobacterium africanum* também podem ser agentes da doença, em uma menor frequência [1,2]. Estas bactérias estão agrupadas no chamado "Complexo" *Mycobacterium tuberculosis* e reúnem espécies de importância médica e veterinária [3]. Estudos mostraram que a TB é uma doença antiga, tendo seus primeiros relatos no Egito Antigo onde foram encontradas lesões típicas da doença em múmias, que datam de pelo menos 6 mil anos atrás [4].

A origem do MTB ainda é incerta. Evidências sugerem que uma bactéria do solo passou a colonizar animais há pelo menos 10 mil anos [5]. Observou-se que todas as espécies de micobactérias adaptadas a animais possuem uma origem comum devido a uma deleção de uma região conhecida por RD9, porém esta mesma região se mantém intacta no MTB [3]. Também observou-se que o *Mycobacterium bovis*, causador de TB em humanos e gado, possui um genoma menor que de MTB, o que eliminaria a possibilidade do bacilo adaptado a humanos ter derivado do adaptado a gado, uma vez que estes bacilos não podem reparar deleções no seu DNA por recombinação homóloga [3].

A epidemia de TB na Europa teve início no começo do século XVII e se estendeu pelos 200 anos seguintes. Após a Revolução Industrial as cidades europeias e americanas proporcionavam um ambiente favorável à disseminação do patógeno pelo ar, uma vez que a densidade populacional era alta e as condições sanitárias precárias. A epidemia se disseminou lentamente para diferentes locais, incluindo a África, devido à exploração e colonização pelos europeus e norte-americanos [2].

Muitos pesquisadores estudaram a TB, tentando encontrar definições para os sintomas, as características e as possíveis causas e formas de contágio, porém apenas em 1882 Robert Koch identificou o MTB como o agente etiológico da doença. O surgimento da vacina BCG (bacilo Calmette-Guérin) ocorreu 39 anos após a identificação do bacilo, e até hoje é a principal estratégia profilática contra a TB. Porém, a BCG não possui uma cobertura

eficiente em adultos, protegendo apenas crianças, destacando a necessidade de busca por novas estratégias [2,6].

Finalmente, a introdução de compostos anti-TB, como estreptomicina (1944), isoniazida (1952), pirazinamida (1952), etambutol (1961) e rifampicina (1966) representaram uma quimioterapia efetiva que reduz drasticamente a mortalidade causada pela TB [4]. Em 1969, a *U.S. Surgeon General* afirmou que era hora de "fechar o livro para as doenças infecciosas" [4].

1.2 Dados atuais sobre TB

Ao contrário do que se imaginou na segunda metade do século XX, a TB não foi erradicada e permanece como uma das principais causas de morte por doenças infecciosas mundialmente, especialmente na Ásia e na África. Estima-se que 8,6 milhões de casos novos e 1,3 milhões de mortes causadas por TB ocorreram no ano de 2011 [8].

Alguns fatores são atribuídos ao retorno dessa doença na população: o aumento da resistência a fármacos, a pandemia do Vírus da Imunodeficiência Humana (HIV), o aumento de usuários de drogas injetáveis, o aumento de imigrantes de países com alta prevalência da doença para países desenvolvidos, o aumento da longevidade da população humana, a ampliação de ambientes com alta aglomeração de pessoas, como por exemplo, prisões, hospitais e abrigos e também a degradação dos sistemas de saúde pública [2]. A TB apresenta índices mais perigosos quando associada com o HIV [8]: pessoas com HIV tem até 34 vezes mais chance de desenvolver TB ativa. Além disso, a TB é a causa da morte de 25% de indivíduos infectados [8,9].

A maior parte dos casos estimados em 2011 está localizada no continente asiático (59%) e africano (26%). Já a região leste do Mediterrâneo, a Europa, e as Américas possuem 7,7%, 4,3% e 3% dos casos, respectivamente (Figura 1). A Índia, a China, a África do Sul, a Indonésia e o Paquistão formam o grupo dos cinco países com o maior número de casos incidentes no mundo. Somente a Índia representa 26% de todos os casos de TB, e quando associada à China, contabilizam 38% dos casos totais. Além disso, 3,7% dos casos novos e 20% de casos previamente tratados são considerados de TB com multirresistência a drogas anti-TB (MDR-TB) [8].

MDR-TB é caracterizada pela resistência às drogas de primeira linha, isoniazida e rifampicina. Pacientes com MDR-TB e co-infectados com HIV são os que possuem pior prognóstico, uma vez que essa associação tem provocado altas taxas de mortalidade, especialmente quando diagnosticada tardiamente [12,16]. Além do mais, nos últimos anos, casos de TB extensivamente resistente a drogas (XDR-TB) têm sido relatados em diversos países [8]. XDR-TB é definida como a condição em que os isolados de TB são resistentes à isoniazida e rifampicina, e pelo menos, uma ou mais das três drogas injetáveis de segunda linha, resultando em opções limitadas de tratamento, além dessas drogas causarem mais danos ao homem [8,17]. Indivíduos infectados com XDR-TB possuem um prognóstico ruim, com altos índices de falha do tratamento e alta mortalidade [16]. As formas de TB resistentes representam, portanto, uma ameaça à saúde pública e ao controle da TB no mundo, aumentando a preocupação em relação à epidemia de TB incurável [18].

Figura 1. Mapa mundial com os casos novos de TB no ano de 2011.

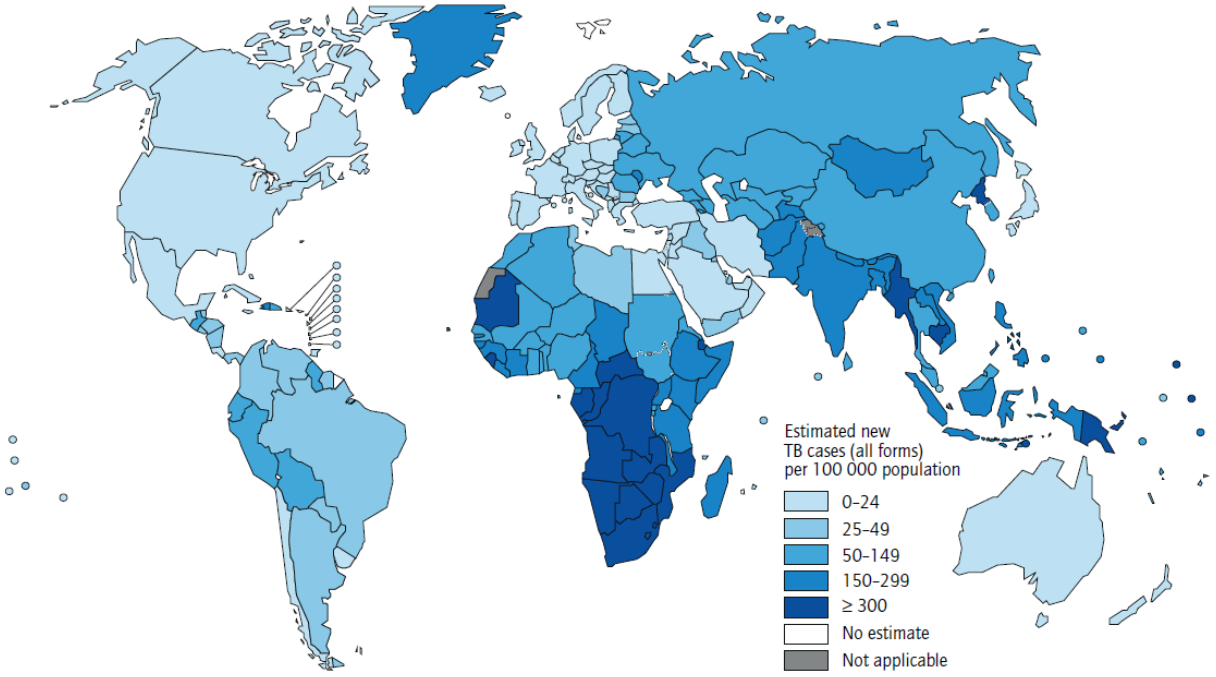

Fonte: WHO (2012).

O Brasil faz parte dos 22 países que correspondem a 80% dos casos mundiais da TB, sendo também priorizado pela Organização Mundial da Saúde (OMS) no combate à doença. Em 2007, 72.194 novos casos foram notificados no país, sendo São Paulo o estado com o maior número absoluto de ocorrências, enquanto que o Rio de Janeiro apresenta a maior

incidência do país [10]. Em 2009, aproximadamente 4.500 pessoas morreram dessa doença no Brasil [8,10].

1.3 Patogenia

A TB pode ser causada por outras espécies de micobactérias (*M. africanum* e *M. bovis*) [2,7]. Porém, o MTB é o principal agente etiológico da doença em humanos, sendo um micro-organismo aeróbio e de crescimento lento. Embora esse patógeno possa infectar diversos órgãos do hospedeiro, a TB pulmonar apresenta-se como a forma mais comum [2,8,11].

A infecção é normalmente adquirida por inalação do bacilo [11,12], através de gotículas que são expelidas da garganta e dos pulmões de indivíduos que possuem a TB pulmonar ativa [8]. As chances de se desenvolver a doença ativa, após inalar gotículas do ar contaminadas com o bacilo, são muito baixas – aproximadamente 5% [13].

Embora a maioria dos bacilos inalada seja rapidamente contida pelo sistema imune, após atingir os pulmões, a bactéria é geralmente fagocitada por macrófagos alveolares e condicionada a um estado de latência, uma vez que essas células são capazes de conter o crescimento, mas não de eliminar o patógeno. Em seguida, outras células do sistema imune do hospedeiro são recrutadas, sendo responsáveis pela resposta inflamatória gerada e pela formação do granuloma, ou tubérculo, a principal característica da TB. Ao contrário da forma ativa, a TB latente não é contagiosa e, na maioria dos casos, os indivíduos infectados com o bacilo não desenvolvem a doença [2,11,14].

A TB ativa ocorre como resultado de uma nova infecção ou reativação da forma latente. A reativação da doença é frequentemente desencadeada por condições que comprometem o sistema imune do paciente, tais como: casos de má nutrição, idade avançada, abuso de drogas, terapia com imunossupressores ou co-infecção com HIV [11,12]. A diminuição da resposta imune desencadeia uma série de eventos que podem levar ao rompimento do granuloma, levando a danos no tecido pulmonar e a disseminação de milhares de partículas infectadas através das vias aéreas [14].

Atualmente, a infecção por HIV representa o maior risco para o desenvolvimento da forma ativa da TB, sendo esta a principal causa de morte devido a doenças infecciosas em

pacientes portadores de HIV [2,8,12]. Casos de TB extrapulmonar, em particular a TB meningítica, são mais comuns na população HIV positiva [12].

Indivíduos infectados com o bacilo, porém saudáveis, geralmente são assintomáticos. Os sintomas da TB pulmonar ativa se manifestam através da tosse, muitas vezes contendo escarro e sangue, dores do peito, fraqueza, perda de peso e sudorese noturna [4,6,12]. No entanto, após 2 a 4 semanas de tratamento apropriado, os sintomas diminuem, induzindo muitos pacientes a interromper a terapia [4].

1.4 Tratamento da Tuberculose

A OMS recomenda o tratamento conhecido como DOTS (do inglês, *Directly Observed* Treatment *Short Course*) [2]. A terapia consiste em uma associação de fármacos de primeira linha, isoniazida, rifampicina, pirazinamida e etambutol durante dois meses, seguida por quatro meses com isoniazida e rifampicina [4,8], tendo sucesso na maioria dos casos [4]. Além disso, a estratégia do DOTS inclui outros 5 componentes: i) estabelecer uma rede de indivíduos treinados a administrar e supervisionar o DOTS; ii) criar laboratórios e profissionais habilitados para o diagnóstico da TB; iii) implementar um sistema de fornecimento confiável de medicamentos de alta qualidade (preferencialmente, sem custo aos pacientes); iv) compromisso governamental e; v) estabelecer um sistema de monitoramento dos casos, tratamento e resultados [6,8]. Essas estratégias podem prevenir a ocorrência de novas infecções e, mais importante, dificultam o surgimento de casos MDR-TB e XDR-TB [2].

A falha do tratamento, definida como a presença de culturas positivas após cinco meses de terapia apropriada, pode ser resultado da falta de adesão pelo paciente devido à sua longa duração e complexidade, possíveis efeitos adversos ou resistência do bacilo às drogas [8,12]. Tais circunstâncias favorecem o surgimento de organismos resistentes aos medicamentos utilizados no esquema terapêutico [4].

Para o desenvolvimento de novas drogas para o tratamento da TB, existem requisitos relevantes: diminuição do tempo de tratamento; capacidade de atingir cepas MDR e XDR; simplificação do tratamento, através da redução das pílulas diárias; e capacidade de ser coadministrados com drogas anti-HIV [13].

A emergência de cepas MDR e XDR, bem como a epidemia de HIV leva a uma necessidade urgente de um melhor entendimento sobre os mecanismos moleculares de ação e de resistência aos fármacos, facilitando a pesquisa por novos compostos anti-TB efetivos tanto no combate da TB suscetível aos fármacos quanto em casos MDR/XDR [2]. O sequenciamento do genoma do MTB permitiu avanços na descoberta de novos alvos para combater a doença [13,19]. No entanto, o sucesso na identificação de novos candidatos a fármacos, baseado no estudo do genoma, ainda é baixo, em parte pela dificuldade em identificar inibidores específicos [13]. Dentro desse panorama, há uma necessidade urgente de desenvolvimento de novos fármacos anti-TB [16].

2. Metabolismo de Nucleotídeos

O estudo da bioquímica básica de um organismo patogênico é o primeiro passo para o desenvolvimento de novos medicamentos contra uma determinada enfermidade causada pelo mesmo [20]. Os nucleotídeos são ésteres de fosfato de um açúcar de cinco átomos de carbono (pentose), nos quais uma base nitrogenada está covalentemente ligada ao C1´ do resíduo de açúcar (Figura 2) [23].

Os nucleotídeos são moléculas orgânicas que participam de diversas funções e processos bioquímicos importantes para os organismos. Estão presentes como unidades monoméricas do DNA e RNA; ATP, GTP e UTP, quando hidrolisados, dirigem processos que requerem energia livre; ATP, ADP e AMP atuam como reguladores de diversas rotas metabólicas; cAMP e cGMP mediam sinalização hormonal; NAD^+, $NADP^+$, FMN, FAD e coenzima A são coenzimas essenciais para uma grande variedade de reações enzimáticas [23]. Quase todos os organismos podem sintetizar nucleotídeos através de duas vias: *de novo* e salvamento, demonstrando sua importância para os processos biológicos [20,21,23].

Figura 2. Estrutura de um ribonucleotídeo.

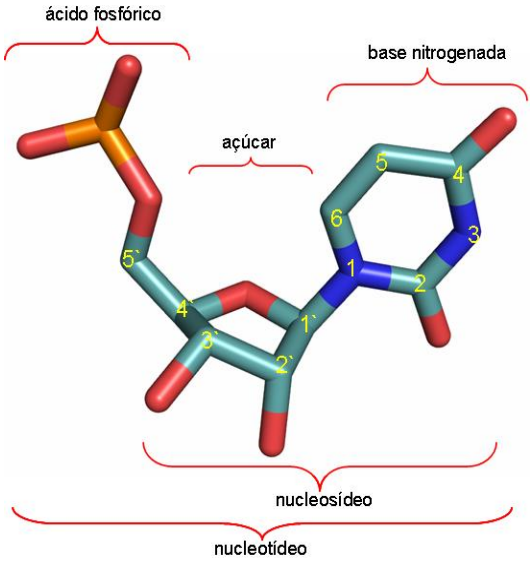

Fonte: VOET & VOET (2006).

Em 1994, o Instituto Nacional de Alergia e Doenças Infecciosas dos EUA lançou um programa de incentivo à pesquisa de novas drogas anti-TB, o qual revelou diversos análogos de purinas que tinham seletividade contra componentes do bacilo da TB [20]. Este fato mostrou que as enzimas envolvidas no metabolismo das purinas podem servir de alvos para o desenvolvimento de novos fármacos com uma alta seletividade.

A formação dos nucleotídeos de purinas pode ocorrer através de uma rota bioquímica chamada de via de salvamento de purinas (Figura 3), onde os nucleotídeos AMP, GMP e IMP podem ser formados a partir das bases livres adenina, guanina e hipoxantina, respectivamente [21], ou através da rota *de novo* (Figura 4), na qual os nucleotídeos são formados a partir de precursores simples.

Figura 3. Via de salvamento de purinas.

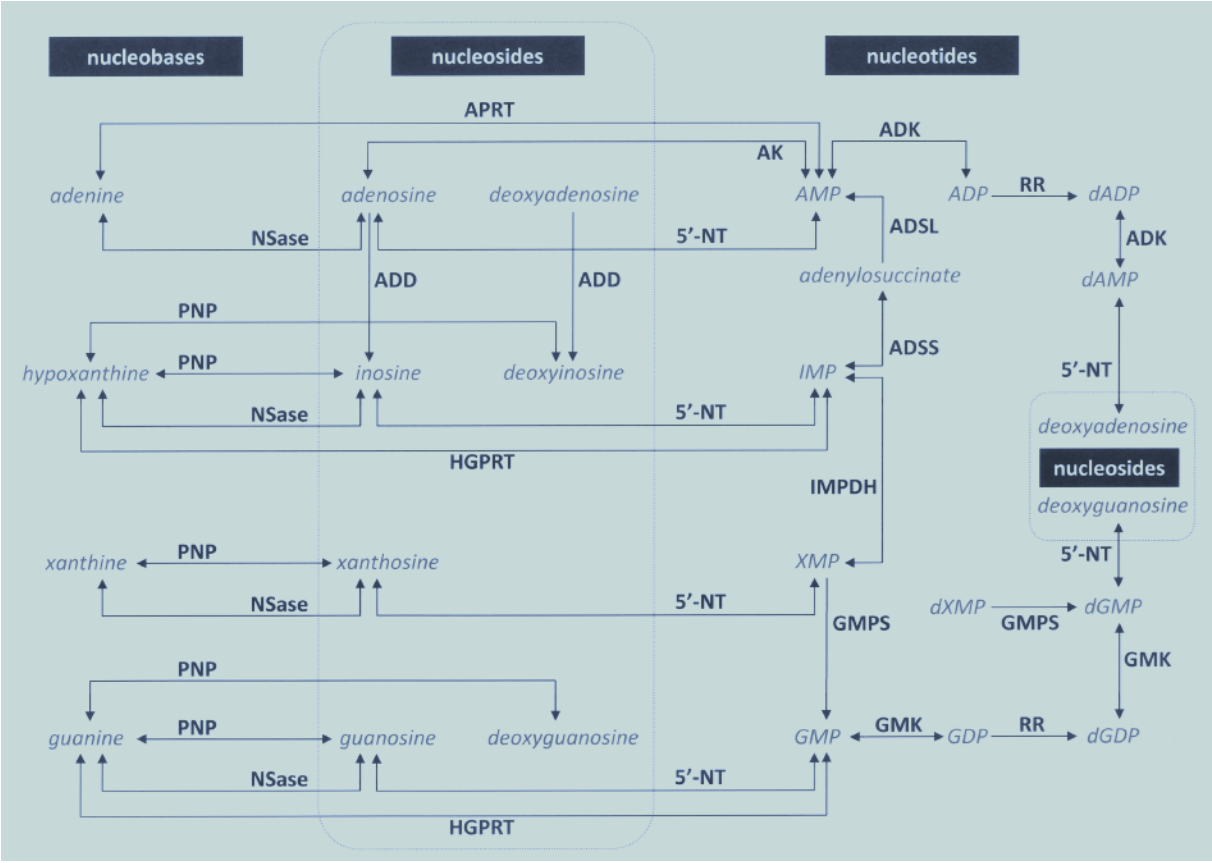

Fonte: DUCATI et al (2011).
Nota: 5'-NT: 5'- Nucleotidase; APRT: Adenina Fosforribosiltransferase; ADK: Adenilato Quinase; AK: Adenosina Quinase; ADSL: Adenilosuccinato Liase; ADSS: Adenilosuccinato Sintase; GMK: Guanosina Monofosfato Quinase; GMPS: Guanosina Monofosfato Sintase; IMPDH: Inosina Monofosfato Desidrogenase; NSase: Purina Nucleotidase; PNP: Purina Nucleosídeo Fosforilase; RR: Ribonucleotídeo Redutase.

Sabe-se que o metabolismo de purinas está presente tanto em seres eucarióticos quanto em seres procarióticos, incluindo o MTB, que expressa as enzimas de ambas as vias metabólicas. Entretanto, não está claro como a micobactéria alterna entre as duas vias. Acredita-se que, em situações de multiplicação rápida ou baixa disponibilidade energética, a bactéria utilize preferencialmente a via de salvamento, visto que a via *de novo* demanda um alto gasto energético, por meio de 11 passos de síntese de nucleotídeos a partir de substratos mais simples. Além disso, sabe-se que o MTB utiliza esta via quando absorve hipoxantina, guanina e adenina do meio externo, convertendo-os nos respectivos nucleotídeos [21].

Figura 4. A via de novo de purinas.

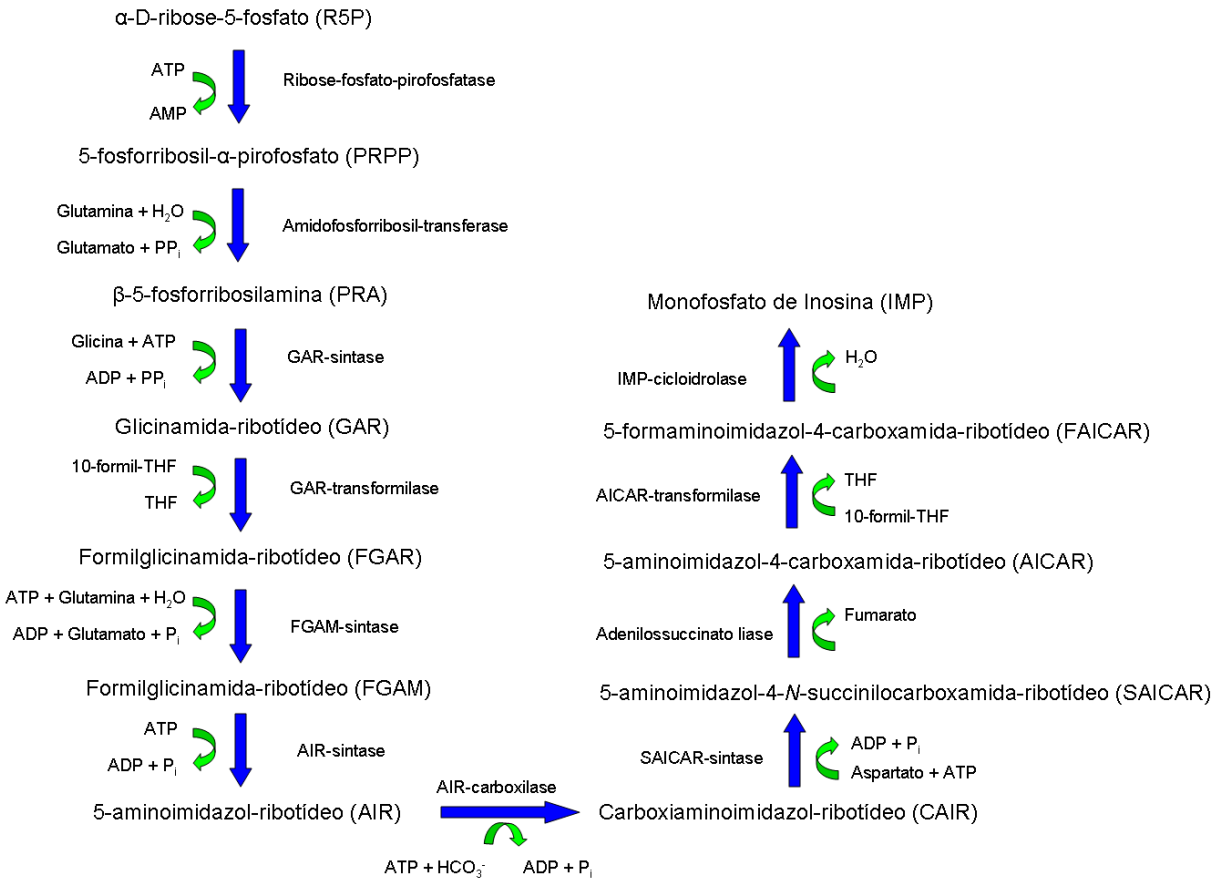

Fonte: Adaptado de VOET & VOET (2006).

3. Hipoxantina-Guanina Fosforribosiltransferase

Em mamíferos e em outros organismos, existem enzimas que participam da via de salvamento de bases, reciclando bases purínicas pré-formadas para que sejam utilizadas no metabolismo celular. Esta via está ativa principalmente durante períodos de rápido crescimento, como, por exemplo, na reprodução assexuada, na embriogênese e na proliferação tumoral [24].

Algumas destas enzimas fazem parte da família do tipo I das fosforribosiltransferases (PRTases), as quais realizam a catálise reversível da transferência de um grupo fosforribosil do composto fosforribosilpirofosfato (PRPP) para uma base purínica livre, como adenina, guanina, hipoxantina e xantina [21].

Apesar da falta de homologia entre as sequencias das PRTases tipo 1, foi proposto que esta família compartilha uma estrutura comum, relacionada com um domínio típico de ligação de nucleotídeos. [25] Apenas uma curta sequencia de aproximadamente 12 aminoácidos é bem conservada entre as PRTases. Esta sequencia, que também é encontrada em PRPP sintase, foi proposta como um motivo de ligação de PRPP. [26]

As reações catalisadas pelas PRTases tipo 1 usualmente seguem um mecanismo sequencial bi-bi ordenado, no qual PRPP se liga a enzima livre, seguido pela base purínica, e após a catálise ocorre a liberação de PPi e o respectivo nucleotídeo. [27-28] Outra característica comum as PRTases tipo 1 é um longo *loop* flexível intimamente associado com o sítio ativo, chamado de "alça catalítica". Na maioria das estruturas determinadas de PRTases tipo 1, a alça é altamente desordenada. [29]

Uma das enzimas PRTases integrante da via de salvamento de bases purínicas, é a hipoxantina-guanina fosforribosiltransferase (HGPRT) [21]. Sua reação envolve a ribofosforilação em uma etapa de nucleobases de purina (hipoxantina ou guanina) para a formação do nucleosídeo 5'-monofosfato e pirofosfato inorgânico (Figura 5). Em MTB a enzima (*Mt*HGPRT) é codificada pelo gene *hpt* e possui 606 pares de bases [21].

Figura 5. Reações reversíveis catalisadas pela HGPRT.

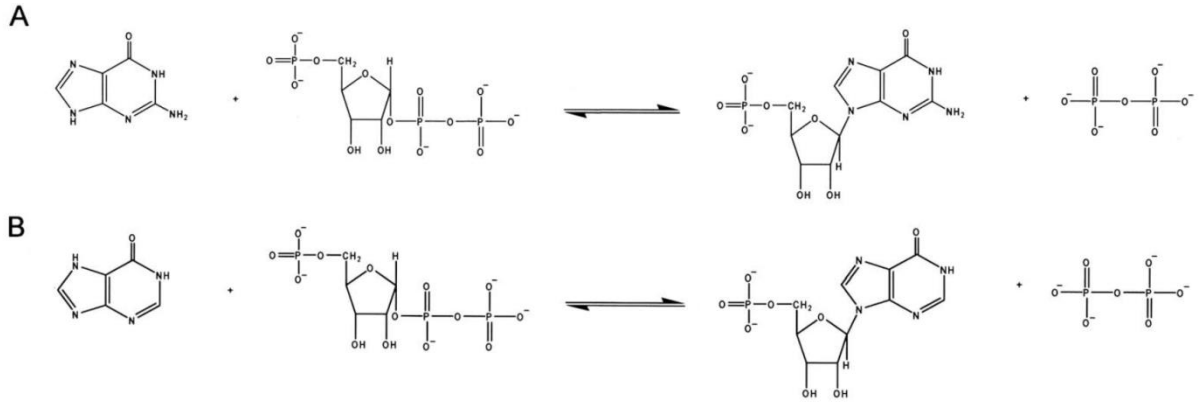

Fonte: Adaptado de BIAZUS et al (2009).
Nota: Reações catalisadas pela HGRPT. A mostra a reação de HPRT e B reação de GPRT.

A HGPRT é uma enzima com uma larga distribuição filogenética, sendo reportada em bactérias gram-negativas e positivas, leveduras, mamíferos e eucariotos basais como os do gênero *Plasmodium* e *Leishmania*. Em humanos, a HGPRT é encontrada no fígado, hemácias

e tecido nervoso [30]. A inexistência de atividade de HGPRT em humanos causa a Síndrome de Lesh-Nyhan, conhecida por hiperuricemia, e desordens neuronais como retardo mental e comportamento auto-mutilatório, porém a deficiência parcial de atividade da enzima leva a um quadro de gota [30]. Muitos organismos que parasitam humanos, como os gêneros *Schistosoma* e *Plasmodium*, não possuem a via *de novo* de purinas, utilizando apenas a via de salvamento tornando, desse modo, a HGPRT um alvo para fármacos [30].

O modo de ação da HGPRT de MTB (*Mt*HGPRT) ainda não está completamente elucidado. Portanto, a investigação da via de salvamento de purinas, incluindo a *Mt*HGPRT, pode revelar propriedades interessantes acerca da complexa relação que existe entre o bacilo e o hospedeiro. [31]

4. Justificativa

O surgimento de diferentes cepas resistentes e os altos índices de infecção e mortalidade no mundo reflete a evidente necessidade de geração de novas formas de compreender e combater a doença. É necessária uma melhoria nas condições do tratamento utilizado atualmente.

O estudo das enzimas e vias metabólicas de MTB permite o entendimento da bioquímica deste patógeno através de estudos cinéticos e termodinâmicos.

Enzimas envolvidas no metabolismo de purinas tornam-se alvos promissores para o desenvolvimento de novas drogas anti-TB e vem sendo muito estudadas, uma vez que essas proteínas são responsáveis pela biossíntese dos precursores do DNA e RNA e, portanto, essenciais à sobrevivência do bacilo [21].

O estudo de seu modo de ação é de grande relevância, uma vez que isto permite conhecer suas propriedades enzimáticas, fornecendo indícios que revelem a importância dessa proteína ao metabolismo do bacilo da TB, permitindo um melhor entendimento desta enzima na via de salvamento de purinas.

5. Objetivos

5.1 Objetivo geral

Este trabalho faz parte de um projeto maior que visa à caracterização de enzimas da via de salvamento de purinas e pirimidinas de *Mycobacterium tuberculosis* como alvos para o desenvolvimento de fármacos para o tratamento da TB, bem como o entendimento do funcionamento destas vias neste microorganismo. Desse modo, serão realizados estudos cinéticos e termodinâmicos para a elucidação do modo de ação da HGPRT deste microorganismo.

5.2 Objetivos específicos

I. Determinar o estado oligomérico em solução da enzima *Mt*HGPRT;

II. Determinar as constantes cinéticas verdadeiras (K_m, V_{max} k_{cat}) para os substratos da enzima *Mt*HGPRT;

III. Determinar os parâmetros termodinâmicos de ligação dos substratos e produtos da enzima *Mt*HGPRT;

IV. Determinar a energia de ativação da enzima *Mt*HGPRT através de ensaios espectrofotométricos variando a temperatura;

V. Realizar experimentos de cinética pré-estacionária para observar a relevância da liberação dos produtos para a etapa lenta nas reações da *Mt*HGPRT;

VI. Realizar estudo de efeitos isotópicos do solvente para avaliar a contribuição da transferência de prótons na etapa lenta nas reações da *Mt*HGPRT;

VII. Determinação da constante de equilíbrio para as reações catalisadas pela enzima *Mt*HGPRT;

VIII. Realização de estudos do efeito do pH na ligação e catálise da enzima *Mt*HGPRT.

CAPÍTULO 2

ARTIGO CIENTÍFICO

Artigo submetido para o periódico Biochemistry (Fator de Impacto 3.4)

Mode of Action of Recombinant Hypoxanthine-Guanine Phosphoribosyltransferase from *Mycobacterium tuberculosis*

Paulo C. Patta,[†,‡] Leonardo K. B. Martinelli,[†] Bruno L. Abbadi ,[†,‡] Diogenes S. Santos,[†,] Luiz A. Basso[†,*]*

[†]Centro de Pesquisas em Biologia Molecular e Funcional (CPBMF), Instituto Nacional de Ciência e Tecnologia em Tuberculose (INCT-TB), Pontifícia Universidade Católica do Rio Grande do Sul (PUCRS), 6681/92-A Av. Ipiranga, 90619-900, Porto Alegre, RS, Brazil. Fax/Tel: +55-51-33203629

[‡]Programa de Pós-Graduação em Biologia Celular e Molecular, Pontifícia Universidade Católica do Rio Grande do Sul (PUCRS), 6681/92-A Av. Ipiranga, 90619-900, Porto Alegre, RS, Brazil. Fax/Tel: +55-51-33203912

KEYWORDS

Type I PRTases, Purine Metabolism, Isothermal Titration Calorimetry, Enzyme Kinetics.

AUTHOR INFORMATION

Corresponding Authors

L. A. Basso or D. S. Santos. E-mails: luiz.basso@pucrs.br or diogenes@pucrs.br. Phone: +55-51-33203629

Author Contributions

The manuscript was written through contributions of all authors. All authors have given approval to the final version of the manuscript.

Notes

The authors declare no competing financial interest.

ABBREVIATIONS

APRTase, adenine phosphoribosyltransferase; CHES, *N*-2-(*N*-Cyclohexylamino)ethanesulfonic acid; CV, column volume; E_a, energy of activation; Gua, guanine; HEPES, *N*-2-Hydroxiethylpiperazine-*N*-2ethanesulphonic acid; HGPRT, hypoxanthine-guanine phosphorybosiltransferase; HIV, human immunodeficiency virus; HMW, high molecular weight; *Hs*HGPRT, *Homo sapiens* HGPRT; Hx, hypoxanthine; GMP, guanosine 5′-monophosphate; IMP, inosine 5′-monophosphate; ITC, isothermal titration calorimetry; K_{eq}, equilibrium constant; LMW, low molecular weight; MES, 2-(*N*-Morpholino)ethanesulphonic acid; *Pf*HGPRT, *Plasmodium falciparum* HGPRT; PNP, purine nucleoside phosphorylase; OPRTase, orotate phosphoribosyltransferase; PPi, inorganic pyrophosphate; PRPP, 5'-phosphoribosyl-α-1'-pyrophosphate; PRTase, purine phosphoribosyltransferases; TB, tuberculosis.

Abstract

Tuberculosis (TB) is an infectious disease caused mainly by *Mycobacterium tuberculosis*. The increasing number of infected patients among immune compromised populations and emergence of drug-resistant strains has created an urgent need of new strategies to treat TB. A better understanding of biochemical pathways (as the purine salvage) can unveil details of the biology of *M. tuberculosis* that might be used to develop new strategies to combat this pathogen. Hypoxanthine-guanine phosphoribosyltransferase (HGPRT) is an enzyme from the purine phosphoribosyltransferase (PRTase) family and catalyzes the conversion of hypoxanthine or guanine and 5-phospho-α-D-ribose 1-diphosphate (PRPP) to, respectively, inosine 5'-monophosphate (IMP) or guanosine 5'-monophosphate (GMP), and pyrophosphate (PPi). Gel filtration chromatography has shown that *M. tuberculosis* HGPRT (*Mt*HGPRT) is a homodimer in solution. A sequential compulsory ordered enzyme mechanism with PRPP as the substrate that binds to free *Mt*HGPRT and PPi as the first product to dissociate is proposed based on kinetic data and thermodynamics of ligand binding from isothermal titration calorimetry (ITC) results. ITC data have also provided thermodynamic signatures of non-covalent interactions for PRPP, IMP and GMP binding to free *Mt*HGPRT. Thermodynamic activation parameters (E_a, $\Delta G^{\#}$, $\Delta S^{\#}$, $\Delta H^{\#}$) for *Mt*HGPRT-catalyzed chemical reaction, pre-steady-state kinetics, solvent kinetic isotope effects, equilibrium constants, pH-rate profiles, and multiple sequencing alignment are also presented. The data here described provide a better understanding of the mode of action of *Mt*HGPRT in the purine salvage pathway, which, in turn, may contribute to better our understanding of the biology of *M. tuberculosis*.

Mycobacterium tuberculosis is the major etiological agent of human tuberculosis (TB) and is believed to infect one-third of the world's population. This bacteria was responsible for 8.6 million new TB cases in 2012, which resulted in 1.3 million deaths worldwide.[1] According to the World Health Organization (WHO), TB is the second most important cause of mortality worldwide due to a single infectious agent.[1] Despite the effective short-course chemotherapy, the increasing global burden of TB has been associated with co-infection with human immunodeficiency virus (HIV)[1,2], emergence of multi, extensively[3] and recently, totally drug resistant strains of *M. tuberculosis*.[4]

TB is an ancient human disease[5], but little is known about the nutritional adaptability of *M. tuberculosis* in the progression of TB infection.[6,7] It is still not clear whether *M. tuberculosis* recycles complex nutrient molecules from the human host using salvage pathways or relies on synthesis of essential molecules from passive diffusible precursors via *de novo* synthesis pathways. Purine and pyrimidine salvage pathways in *M. tuberculosis* remain an incompletely explored possibility for drug development as purine and pyrimidine biosynthesis are essential steps for the cell, supplying building blocks for DNA and RNA synthesis, among other biological roles.[8] Accordingly, elucidation of biochemical properties of the enzymes involved in purine and pyrimidine salvage pathways should contribute to a better understanding of the biology of *M. tuberculosis*, and, hopefully, to the design of analogs that may selectively inhibit *M. tuberculosis* replication and survival.[9]

The purine phosphoribosyltransferases (PRTases) form a family of enzymes that transfer pyrophosphate (PPi) from 5-phospho-α-D-ribose 1-diphosphate (PRPP; α-D-5-phosphoribosylpyrophosphate; α-D-ribosyl diphosphate 5-phosphate) to a nitrogen-containing nucleophile (such as the imidazole N-9 of a purine base) to form the corresponding β-substituted ribose 5-phosphate (such as purine nucleotides).[10] Despite the lack of clear sequence homology among the PRTases, these enzymes show tertiary and quaternary

structure conservation.[11] A PPRP binding motif of 12 amino acids, which is also found in PRPP synthetases, is conserved among the PRTases involved in nucleotide synthesis or salvage pathways.[12] This is the main unifying characteristic of type I PRTases. The type I purine PRTase-catalyzed reactions have been found to follow a sequential ordered bi-bi mechanism, in which PRPP binds to the free enzyme followed by the purine base, and ordered PPi and nucleotide products release.[13-16] Another characteristic feature among the type I PRTase structures is a long flexible loop closely associated with the active site, known as "the catalytic loop". In most of the determined structures of type I PRTase, the loop is usually highly disordered.[10] This PRTase family is of significant interest in both human genetic diseases and parasitic pathologies, such as Lesch–Nyhan syndrome and Chagas' disease.[17-18]

One of the enzymes that belongs to this family is the hypoxanthine–guanine phosphoribosyltransferase (HGPRT; EC 2.4.2.8) of purine salvage pathway. HGPRTs are found in most microorganisms and mammals and their reaction involves the ribophosphorylation in one step of purine nucleobases (hypoxanthine and guanine) and their analogues to their respective nucleoside 5'-monophosphate and pyrophosphate.[19] HGPRT catalyzes the Mg^{2+}-dependent reversible transfer of the 5-phosphoribosyl group from PRPP to the N9 of guanine (Gua) (GPRT reaction) or hypoxanthine (Hx) (HPRT reaction) to form the corresponding ribonucleotides guanosine 5'-monophosphate (GMP) and inosine 5'-monophosphate (IMP), releasing PPi.[19] Investigation of purine salvage pathway enzymes of ***M. tuberculosis***, including HGPRT, might reveal insightful data on the complex balance that exists between the bacillus and the host.[19] Accordingly, efforts to elucidate the mode of action of *M. tuberculosis* H37Rv HGPRT (*Mt*HGPRT) appear to be warranted to improve our understanding of purine metabolism in this human pathogen.

The present work describes the mode of action of recombinant *Mt*HGPRT. True steady-state kinetic parameters and isothermal titration calorimetry (ITC) data indicate that *Mt*HGPRT follows a sequential ordered mechanism. Gel filtration data suggest a homodimeric quarternary structure for *Mt*HGPRT. Thermodynamic activation parameters (E_a, $\Delta G^{\#}$, $\Delta S^{\#}$, $\Delta H^{\#}$) for *Mt*HGPRT-catalyzed chemical reaction, solvent kinetic isotope effects, equilibrium constant (K_{eq}) determination, solvent kinetics isotope effects, transient kinetics measurements, pH-rate profiles, and multiple sequencing alignment results are also presented. The absolute requirement of divalent magnesium ion for catalysis, the sequential kinetic mechanism, the presence of PRPP binding motif, the homodimeric assembly in solution indicate that *Mt*HGPRT belongs to type I PRTases family of enzymes.

It is hoped that the results presented here contributes to a better understanding of *Mt*HGPRT mode of action, and may also be useful to chemical biologists interested in designing loss-of-function (inhibitors) or gain-of-function (activators) chemical compounds to reveal the biological role of *Mt*HGPRT in the context of whole *M. tuberculosis* cells.

Materials and Methods

Materials. All chemicals were purchased from Sigma-Aldrich (Saint Louis, USA), unless otherwise specified. The LMW and HMW Gel Filtration Calibration Kits were purchased from GE Healthcare. All kinetic data analyses were carried out using SigmaPlot 10.0 (Systac Software, Inc., Melbourne, USA). ITC data analysis was evaluated utilizing the Origin 7 SR4 software (Microcal, Inc.) All experiments were performed at 25 °C using 50 mM 2-amino-2-hydroxymethyl-propane-1,3-diol (Tris)-HCl pH 7.4 containing 12 mM $MgCl_2$ (buffer A) unless otherwise specified.

Overexpression and Purification. The recombinant *Mt*HGPRT was overexpressed and purified to homogeneity as previously described.[19]

Oligomeric State Determination. The oligomeric state of homogenous *Mt*HGPRT in solution was determined by size exclusion liquid chromatography on a HighLoad 10/30 Superdex-200 column (GE Healthcare). The column was pre equilibrated and the sample (100 μL) was isocratically eluted with 1 column volume (CV) of 50 mM Tris-HCl pH 7.5 containing 200 mM NaCl at a flow rate of 0.4 mL min^{-1}. Protein elution was monitored at 215, 254, and 280 nm. The LMW and HMW Gel Filtration Calibration Kits were used as described by the manufacturer to prepare the calibration curve. The elution volumes (V_e) of protein standards were used to calculate their corresponding partition coefficients (K_{AV}) according to **Eq. 1**. Blue dextran 2000 (GE Healthcare) was used to determine the void volume (V_0) and V_t is the total bead volume of the column. The K_{av} value for each protein was plotted *versus* the logarithm of their corresponding molecular masses, giving a linear relationship. A volume of 100 μL (100 μM) of *Mt*HGPRT was loaded into the gel filtration

column to obtain V_e. The partition coefficient (K_{AV}) of the recombinant *Mt*HPRT was calculated by data fitting to **Eq. 1** and its molecular mass derived from the linear relationship.

$$K_{AV} = \frac{V_e - V_o}{V_t - V_o} \qquad \text{Eq. (1)}$$

Steady-state Kinetics. Recombinant *Mt*HGPRT enzyme activity was measured by a continuous spectrophotometric assay measuring the linear increase in absorbance as a function of IMP or GMP formation in quartz cuvettes (1 cm). The experiments were performed in a UV-visible Shimadzu spectrophotometer UV2550 equipped with a temperature-controlled cuvette holder. The kinetic properties of *Mt*HGPRT for Hx, Gua, and PRPP were spectrophotometrically determined using the difference in molar absorptivity between the nucleotide monophosphate and the free base as described for *Homo sapiens* HGPRT ($\Delta\varepsilon$ = 1900 M^{-1} cm^{-1} at 245 nM for IMP conversion to Hx; and $\Delta\varepsilon$ = 5900 M^{-1} cm^{-1} at 257.5 nm for GMP conversion to Gua).[15] Initial steady-state rates were calculated from the linear portion of the reaction curve under experimental conditions in which less than 5% of the substrate was consumed. True steady-state kinetics parameters were determined from initial velocity measurements for HPRT reaction varying concentrations of Hx (10 – 150 μM) at varied-fixed PRPP concentrations (200 – 4000 μM). For GPRT reaction initial velocity measurements were determined varying concentrations of Gua (10 – 120 μM) at varied-fixed PRPP concentrations (200 – 3600 μM). All reactions started with addition of recombinant *Mt*HGPRT, and all measurements were performed at least in duplicates. Hyperbolic saturation curves of initial rate data at single concentration of the fixed substrate and varying concentrations of the other were fitted to the Michaelis-Menten equation[20] (**Eq. 2**), in which *v*

is the initial velocity, V is the apparent maximum initial velocity, A is the varying substrate concentration and K_m represents the apparent Michaelis-Menten constant.

$$v = \frac{VA}{K_m + A} \qquad \text{Eq. (2)}$$

The k_{cat} values were calculated from **Eq. 3**, in which $[E]_t$ corresponds to the total concentration of enzyme subunits.

$$k_{cat} = \frac{V}{[E]_t} \qquad \text{Eq. (3)}$$

Data from initial velocity measurements showing a pattern of lines intersecting to the left of the *y*-axis in the double-reciprocal plots (or Lineweaver–Burk plot) were fitted to **Eq. 4**, which describes a sequential substrate binding and ternary complex formation.

$$v = \frac{VAB}{K_{ia}K_b + K_aB + K_bA + AB} \qquad \text{Eq. (4)}$$

For **Eq. 3**, v is the initial velocity, V is the true maximum initial velocity, A and B are the concentrations of the substrates, K_a and K_b are their respective Michaelis constants, and K_{ia} is the dissociation constant for enzyme-substrate A binary complex formation.

Isothermal Titration Calorimetry. ITC experiments were carried out using an iTC_{200} Microcalorimeter (Microcal, Inc., Pittsburgh, USA). The instrument reference cell (200 μL)

was loaded with Milli-Q water in all experiments and sample cell (200 μL) was filled with either 100 μM or 80 μM of recombinant *Mt*HGPRT. The injection syringe (39.7 μL) was filled with substrates or products at different concentrations: Hx (7 mM), PRPP (10 mM), IMP (5 mM), GMP (2.5 mM) and PPi (1 mM), and the ligand isotherms were measured by direct titration (ligand into macromolecule). The same buffer preparation was used to dissolve all ligands. The stirring speed was 500 RPM at 25 °C with constant pressure for all ITC experiments. The binding reaction started with one injection of 0.5 μL of ligand to prevent artifacts, followed by 19 injections of 2.0 μL each at 300 s intervals. Control titrations (ligand into buffer) were performed in order to subtract the heats of dilution and mixing for each experiment prior to data analysis. The heat variation was monitored inside the cell allowing determination of binding enthalpy of the process (ΔH) and the equilibrium association constant (K_a). The Gibbs free energy (ΔG) and the entropy (ΔS) of binding were calculated using the relationship described in **Eq. 5**, in which R is the gas constant (8.324 J K^{-1} mol^{-1} or 1.987 cal K^{-1} mol^{-1}), and T is the temperature in Kelvin (T = °C + 273.15).

$$\Delta G = -RT \ln K_a = \Delta H - T\Delta S \qquad \text{Eq. (5)}$$

Pre-Steady State Kinetics. Pre-steady-state kinetic measurements of the reaction catalyzed by *Mt*HGPRT were performed to assess whether or not product release is part of the rate-limiting step. The measurements were carried out using an Applied Photophysics SX.18MV-R stopped-flow spectrofluorimeter on absorbance mode. The increase in absorbance was monitored at 245 nm for HPRT reaction and 257.5 nm for the GPRT reaction for a period of 10 seconds (1 mm split width = 4.65 nm spectral band). The experimental conditions were 5 μM *Mt*HGPRT, 12 mM $MgCl_2$, 500 μM Hx or 250 μM Gua, and 10 mM PRPP (mixing chamber concentrations). The control experiments were performed as the experimental

conditions above in the absence of one compound (*Mt*HGPRT, PRPP, Hx or Gua). The dead time of the stopped-flow equipment is 1.37 ms. The pre-steady-state time course of the reaction was fitted to **Eq. 6** for a single exponential increase (appearance of product), in which A is the absorbance at time t, A_0 is the absorbance at time zero, and k is the apparent first-order rate constant for product formation.[21]

$$A = A_0\left(1 - e^{-kt}\right) \qquad \text{Eq. (6)}$$

Energy of Activation. In order to access the energy of activation (E_a) of the *Mt*HGPRT for HPRT reaction, initial velocities were measured in the presence of saturating concentrations of Hx (150 μM) and PRPP (4000 μM). For GPRT reaction the concentrations were Gua (120 μM) and PRPP (3600 μM). The measurements were made at temperatures ranging from 15 °C to 35 °C (from 288.15 to 308.15 K). *Mt*HGPRT was incubated for several minutes at all temperatures tested and assayed under standard conditions (buffer A) to ensure enzyme stability. The E_a was calculated from the slope (E_a/R) of the Arrhenius plot fitting the data to **Eq. 7**, in which R is the gas constant (8.314 J mol^{-1} K^{-1}) and the constant A represents the product of the collision frequency (Z) and a steric factor (p) based on the collision theory of enzyme kinetics.[22] Here, it is assumed a simplistic view to explain a complex phenomenon and that A id independent of temperature.

$$\ln k_{cat} = \ln A - \left(\frac{E_a}{R}\right)\frac{1}{T} \qquad \text{Eq. (7)}$$

The enthalpy ($\Delta H^{\#}$), entropy ($\Delta S^{\#}$), and Gibbs free energy ($\Delta G^{\#}$) of activation were estimated using **Eqs. 8, 9 and 10** derived from the transition state theory of enzymatic reactions:[22]

$$\Delta H^{\#} = E_a - RT \qquad \text{Eq. (8)}$$

$$\Delta G^{\#} = RT\left(\ln \frac{k_B}{h} + \ln T - \ln k_{cat} \right) \qquad \text{Eq. (9)}$$

and

$$\Delta S^{\#} = \frac{\Delta H^{\#} - \Delta G^{\#}}{T} \qquad \text{Eq. (10)}$$

Energy values are in kJ mol^{-1}, with k_{cat} in s^{-1}, to conform to the units of the Boltzmann (1.3805×10^{-23} J K^{-1}) and Planck (6.6256×10^{-34} J s^{-1}) constants, and R is as for **Eq. 5**. Errors on $\Delta G^{\#}$ were calculated using **Eq. 11**.[22]

$$(\Delta G)_{Err} = \frac{RT(k_{cat})_{Err}}{k_{cat}} \qquad \text{Eq. (11)}$$

Solvent Kinetic Isotope Effects. Solvent kinetic isotope effects were determined by measuring initial velocities for HPRT reaction using a saturating level of one substrate (Hx = 120 μM; PRPP = 4 mM) and varying concentrations of the other (Hx: 10 - 120 μM; PRPP: 0.32 - 4 mM) in either H_2O or 90% D_2O. For GPRT reaction initial velocities measurements were assayed at saturating concentration of one substrate (Gua = 50 μM; PRPP = 4 mM) and varying concentrations of the other (Gua: 10 - 50 μM; PRPP: 0.32 - 4 mM) in either H_2O or 90% D_2O. Data were fitted to **Eq. 12**, which assumes isotope effects on both *V/K* and *V*. In

this equation, $E_{V/K}$ and E_V are the isotope effects minus 1 on V/K and V, respectively, and F_i is the fraction of isotopic label in substrate A.[23]

$$v = \frac{VA}{K(1+F_iE_{V/K}) + A(1+F_iE_V)} \qquad \text{Eq. (12)}$$

Determination of Equilibrium Constant. To determine whether or not *Mt*HGPRT-catalyzed chemical reactions are favorable processes, the equilibrium constants (K_{eq}) were identified at the point of equilibrium between substrates (Hx or Gua, and PRPP) and products (IMP or GMP, and PPi) for, respectively, HPRT and GPRT reactions. The K_{eq} was measured by fixing the ratio of [IMP/Hx] or [GMP/Gua] at 1 and varying the ratio of [PPi/PRPP]. For HPRT reaction, the range of [PPi/PRPP] was from 0.0033 to 0.02 (PRPP: 1000 - 6000 μM; PPi = 20 μM). For GPRT reaction, the range of [PPi/PRPP] was from 0.0066 to 0.025 (PRPP: 800 - 3000 μM; PPi = 20 μM). Specific activities (*y-axis*) were plotted against the ratios (*x-axis*) and fitted to a linear equation. The point at which the curve crosses the abscissa is equal to K_{eq} (no net enzyme-catalyzed chemical reaction). The values for the standard Gibbs free energy ($\Delta G°$) for *Mt*HGPRT-catalyzed chemical reactions were calculated from **Eq. 13**, using the experimentally determined K_{eq} values, the gas constant (R) and absolute temperature in Kelvin (T).

$$\Delta G^0 = -RT \ln K_{eq} \qquad \text{Eq. (13)}$$

pH-rate Profiles. Prior to performing the pH-rate profiles, the recombinant enzyme stability was assessed over a wide pH range (4.5 – 10.5) by incubation for 2 min at 25 °C in 100 mM 2-(*N*-Morpholino)ethanesulphonic Acid (MES)/*N*-2-Hydroxiethylpiperazine-*N*-

2ethanesulphonic Acid (HEPES)/*N*-2-(*N*-Cyclohexylamino)ethanesulfonic Acid (CHES) buffer mixture, and then monitoring its activity in buffer A.[23] The dependence of steady-state kinetic parameters on pH was determined by measuring initial velocities in the presence of varying concentrations of one substrate and saturating level of the other, in 100 mM MES/HEPES/CHES buffer, over the following pH range: for HPRT reaction, 5.5 – 10 (10 – 120 μM varying concentrations of Hx and fixed concentration of PRPP at 4 mM, and 0.4 – 7 mM varying PRPP and fixed concentration of Hx at 120 μM); and for GPRT reaction, 5 – 5.5 (5 – 70 μM varying concentrations of Gua and fixed concentration of PRPP at 4 mM, and 0.65 – 4 mM varying PRPP and fixed concentration of Gua at 70 μM) and 6 – 10 (5 – 35 μM varying concentrations of Gua and fixed concentration of PRPP at 3 mM, and 0.32 – 3 mM varying PRPP and fixed concentration of Gua at 35 μM). All measurements were performed at least in duplicates.

The pH-rate profile was generated by plotting logarithm value of k_{cat} or k_{cat}/K_m of the substrates versus the pH values (5.5 to 10) and data were fitted to **Eq. 14**, in which y is the apparent kinetic parameter, C is the pH-independent plateau value of y, H is the hydrogen ion concentration, and K_a is the apparent acid dissociation constant for the ionizing group.

$$\log V = \log\left(\frac{C}{1+\frac{H}{K_a}}\right) \qquad \text{Eq. (14)}$$

Results

Oligomeric State Determination. In order to determine the oligomeric state of the enzyme, *Mt*HGPRT was loaded on a Superdex 200 HR 10/30 size exclusion column (100 μM). The elution profile of the protein pointed to an apparent molecular mass of 46 kDa, according to data fitting to **Eq. 1**. This value and the *Mt*HGPRT subunit molecular mass value (22.251 kDa) indicates that *Mt*HGPRT has a homodimeric quaternary structure in solution in the protein concentration tested.

Steady-State Kinetics. The initial velocity experiments allowed the calculation of the true steady-state kinetics parameters of the enzyme. The double-reciprocal plots showed a pattern of lines intersecting to the left of the *y*-axis (data not shown). The true macroscopic steady-state kinetic constants for the forward reaction of *Mt*HGPRT are summarized in **Table 1**.

Table 1. *Steady-State Kinetic Parameters for MtHGPRT*

Substrate	K_m (μM)	V_{max} (U mg^{-1})	k_{cat} (s^{-1})	k_{cat}/K_m (M^{-1} s^{-1})
Hypoxanthine	26 ± 2	2.40 ± 0.09	0.89 ± 0.04	3.4 (± 0.3) × 10^{+4}
PRPP[a]	14.1 (± 0.4) × 10^{+2}	-	-	6.3 (± 0.5) × 10^{+2}
Guanine	10 ± 1	0.52 ± 0.01	0.193 ± 0.004	1.9 (± 0.2) × 10^{4}
PRPP[b]	6.5 (± 0.7) × 10^{+2}	-	-	2.9 (± 0.3) × 10^{+2}

[a]HPRT reaction; [b]GPRT reaction

Isothermal Titration Calorimetry. As double reciprocal plots suggested a sequential kinetic mechanism, substrate(s) and product(s) binding processes were assayed by ITC at 25°C to ascertain the order, if any, of chemical compound addition. The measure of heat taken up or released upon binding of a ligand provides the binding enthalpy (ΔH) of the process, an estimate for the stoichiometry of the interaction (n) and the equilibrium binding constant (K_a). These values allow the Gibbs free energy (ΔG) and the entropy (ΔS) of the process to be calculated, as well as the dissociation constant at equilibrium (K_d) from reciprocal of K_a. The

ITC data for binding of ligands to *Mt*HGPRT are summarized in **Table 2**. These binding assays showed that PRPP, IMP and GMP can bind to free *Mt*HGPRT (**Fig. 1 A,B,C**). ITC data for these compounds were fitted to one set of sites model. No significant heat change upon titration of Hx and PPi to *Mt*HGPRT was detected under the experimental conditions for ITC measurements (data not shown).

Table 2. *Binding parameters for MtHGPRT from ITC titration assays.*

	PRPP	GMP	IMP
ΔG (kcal mol^{-1})[a]	-5.9 (± 0.1)	-7.7 (± 0.1)	-5.3 (± 0.2)
ΔS (cal mol^{-1} K^{-1})	20.5 (± 0.4)	-3.94 (± 0.03)	-38 (± 2)
ΔH (kcal mol^{-1})	0.205 (± 0.004)	-8.9 (± 0.1)	-16.7 (± 0.9)
K_a (M^{-1})	2.2 (± 0.3) × 10^{+4}	4.8 (± 0.5) × 10^{+5}	7 (± 1) × 10^{+3}
K_d (µM)	48 (± 7)	2.1 (± 0.2)	1.3 (± 0.2) × 10^{+2}

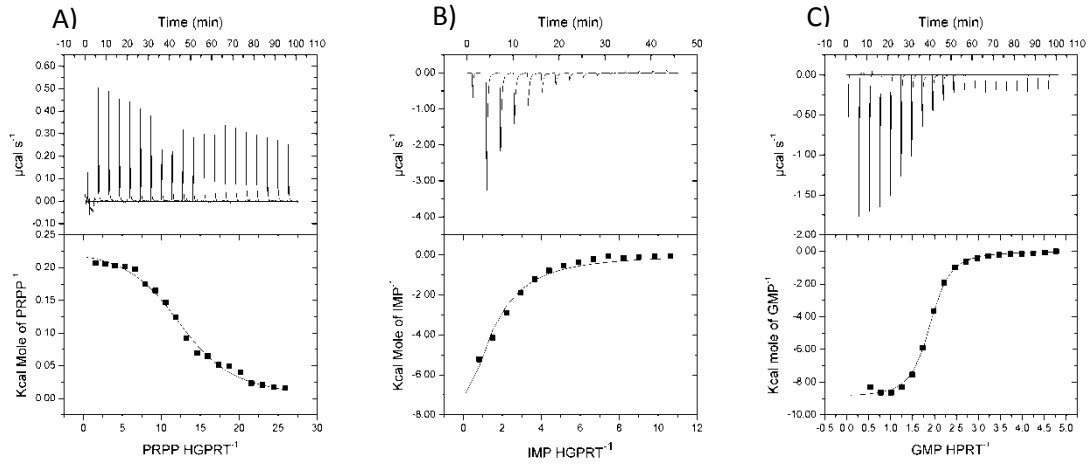

Figure 1. Ligand binding assays for binary complex formation: PRPP (A), IMP (B) and GMP (C) ITC data were fitted to one set of sites binding model.

Pre-Steady-State Kinetics. To determine whether product release contributes to the rate limiting step, pre-steady-state analysis of the reaction catalyzed by *Mt*HGPRT was performed. Fitting the pre-steady-state data to **Eq. 6**, which describes a single exponential increase in absorbance (product formation), yielded a value of 0.213 (± 0.002) s^{-1} for the apparent first-order rate constant for HPRT reaction (**Fig.2 A**), and a value of 0.216 (± 0.001) s^{-1} for GPRT reaction (**Fig. 2 B**).

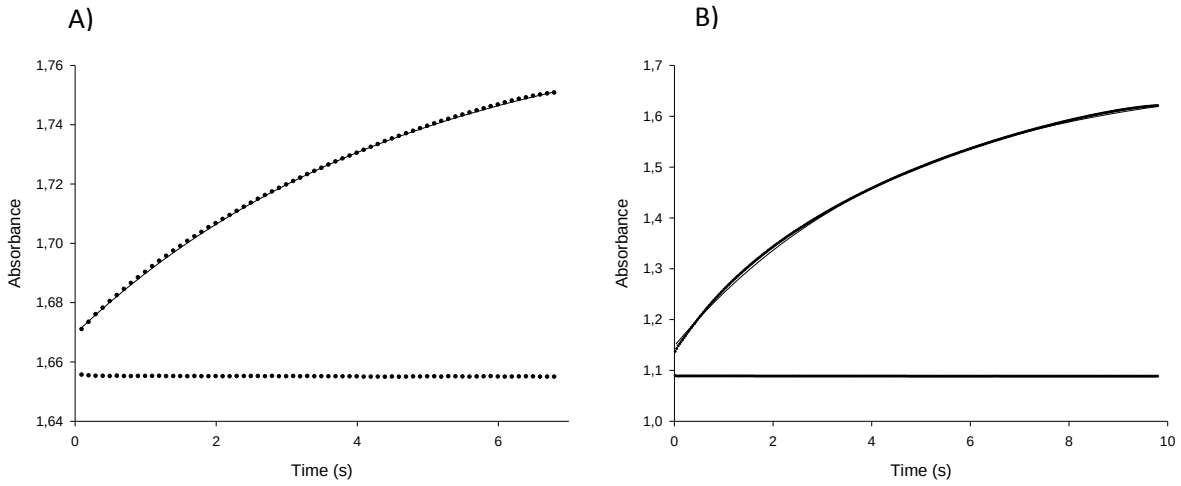

Figure 2. Stopped-flow trace for product formation by measuring the increase in absorbance at 245 nm for HPRT (A) and 257.5 nm for GPRT (B) reactions. Data were fitted to **Eq. 6** for a single exponential increase.

Energy of Activation. The energy of activation for the enzyme-catalyzed chemical reaction was assessed by measuring the dependence of k_{cat} on temperature for Hx and Gua (**Fig. 3**). These data were fitted to **Eq. 7**. The results presented in **Table 3** are derived from data fitting to Equations 7-11. These results provide the energy of activation (E_a), which represents the minimal amount of energy necessary to initiate the chemical reaction catalyzed by *Mt*HGPRT, as well as the transition state enthalpy ($\Delta H^{\#}$), entropy ($\Delta S^{\#}$) and Gibbs free energy ($\Delta G^{\#}$).

Table 3. *Thermodynamic activation parameters for MtHGPRT*[a]

Parameter	HPRT	GPRT
E_a (kcal mol^{-1})	6.20 ± 0.09	5.10 ± 0.03
$\Delta H^{\#}$ (kcal mol^{-1})	5.60 ± 0.08	4.50 ± 0.02
$\Delta S^{\#}$ (cal mol^{-1} K^{-1})	-39.6 ± 0.5	-46.6 ± 0.2
$\Delta G^{\#}$ (kcal mol^{-1})	17 ± 0.2	18 ± 0.1

[a] All values were determined at 25 °C (298.15 K).

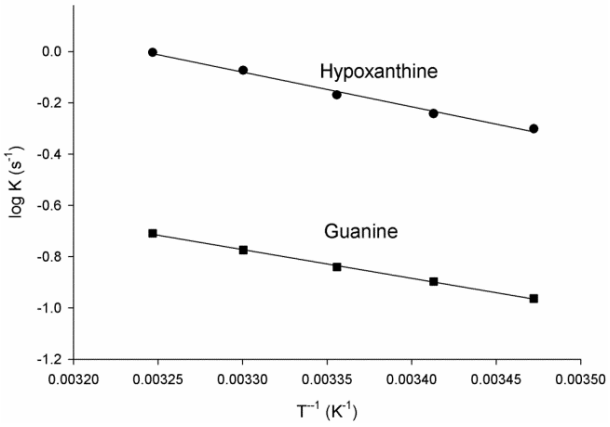

Figure 3. Arrhenius plot for Hx and Gua substrates (temperature dependence of logk_{cat}).

Solvent Kinetic Isotope Effects. To evaluate the contribution of proton transfer from the solvent to the rate of phosphorybosyl transfer of *Mt*HGPRT-catalyzed reaction, solvent kinetic isotope effects were determined by fitting data to **Eq. 12**. The results are given in **Table 4**.

Table 4*. Solvent kinetic isotope effect for MtHGPRT.*

Parameter	Solvent Kinetic Isotope Effect	Comments
$^{D2O}V_{PRPP}$	1.23 ± 0.10	HPRT
$^{D2O}V/K_{PRPP}$	1.29 ± 0.24	HPRT
$^{D2O}V_{Hx}$	1.09 ± 0.08	HPRT
$^{D2O}V/K_{Hx}$	1.26 ± 0.27	HPRT
$^{D2O}V_{PRPP}$	0.71 ± 0.04	GPRT
$^{D2O}V/K_{PRPP}$	0.86 ± 0.19	GPRT
$^{D2O}V_{Gua}$	0.92 ± 0.07	GPRT
$^{D2O}V/K_{Gua}$	0.78 ± 0.34	GPRT

Determination of Equilibrium Constant. Plotting the *Mt*HGPRT enzyme activity as a function of [PPi]/[PRPP] ratio gives a straight line for HPRT and GPRT reactions (**Fig. 4**). This analysis yielded values of 0.0271 for K_{eq} of Hx and 0.0357 for K_{eq} of Gua.

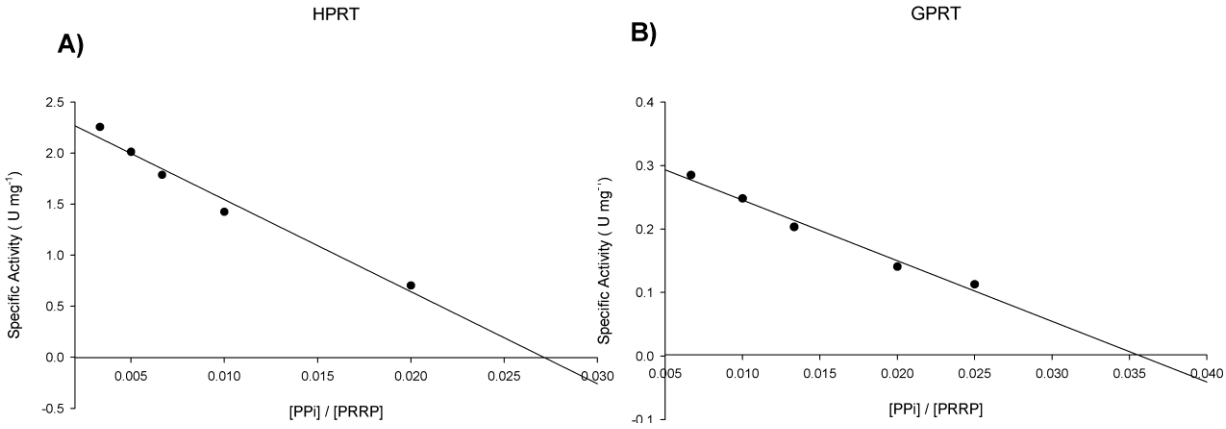

Figure 4. Plot of enzyme activity against different [PPi]/[PRPP] ratios to determine the equilibrium constant for HPRT (A) and GPRT (B) reactions. The ratios for [IMP]/[Hx] and [GMP]/[Gua] were fixed at 1.

pH-rate Profiles. To probe for acid-base catalysis and likely residues involved in catalysis and/or substrate binding, pH-rate profiles were determined for the steady-state kinetic parameters of *Mt*HGPRT. In this experiment, initial velocities measurements were assayed in a broad range of pH values. The pH-rate profiles are shown in **Fig. 5**. Data from the pH-rate profile of HPRT reaction for k_{cat} and k_{cat}/K_{PRPP} were fitted to **Eq. 14**, yielding values of, respectively, 6.3 (± 1.2) and 7.0 (± 0.9) (**Fig. 5A**). For the GPRT reaction, data fitting to **Eq. 14** yielded a value of 6.1 (± 2.8) for k_{cat}/K_{PRPP} and 6.8 (± 2.0) for k_{cat}/K_{Gua} (**Fig. 5B**). There appears to be no obvious ionizing group to be predicted from the k_{cat}/K_{Hx} data for HPRT reaction, and, interestingly, k_{cat} data for GPRT reaction (**Fig. 5A,B**).

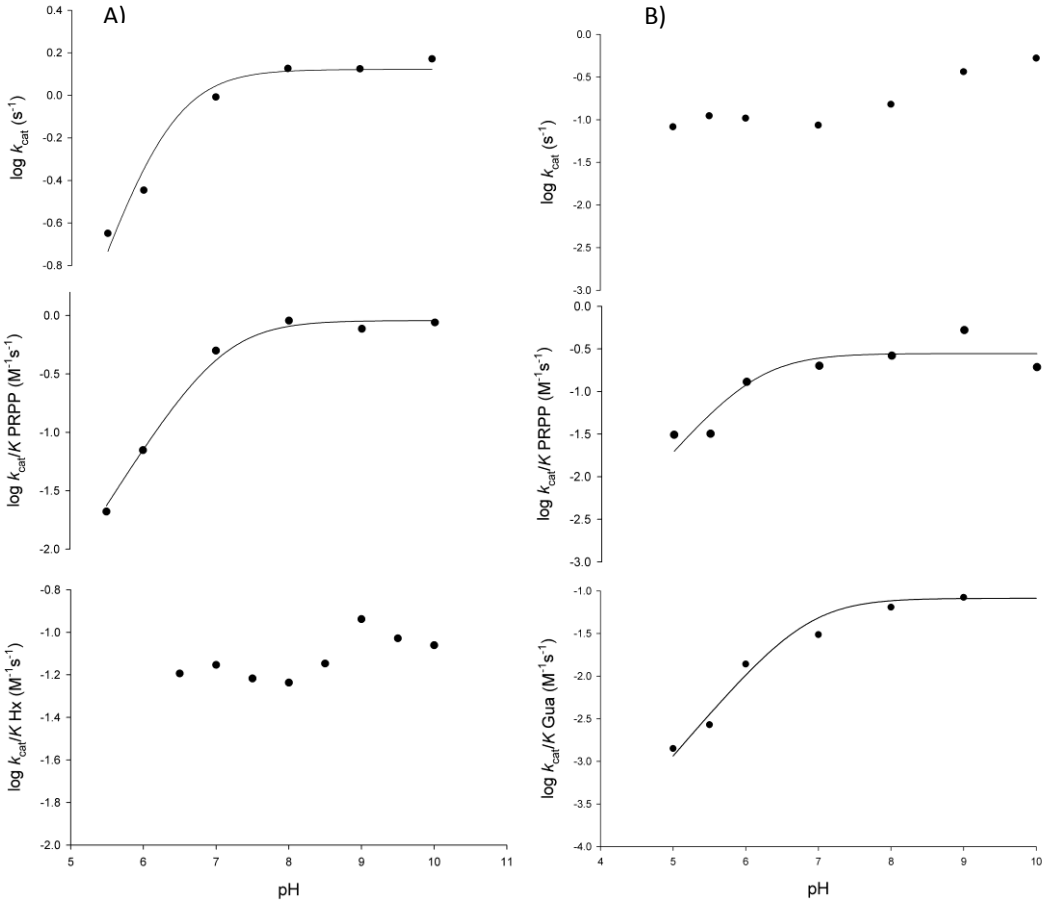

Figure 5. Dependence of steady-state kinetic parameters on different pH values for HPRT (A) and GPRT (B) reactions.

Discussion

Oligomeric State Determination. The size exclusion chromatography results indicate that *Mt*HGPRT is a homodimer of approximately 46 kDa in solution, which suggests that this enzyme belongs to type I PRTases, as this family of enzymes are homodimers.[24]

Steady-state Kinetics. Divalent metal ion activation of substrate PRPP has already been demonstrated as essential for PRTase catalyzed reactions[25-27] in which the dimagnesium Mg_2:PRPP complex (and not PRPP alone) was proved to be the true substrate for HGPRT reaction.[27] No activity could be detected when Mg^{2+} was omitted from the reaction mixture for the *Mt*HGPRT (data not shown). These results are in agreement with *Mt*HGPRT belonging to type I PRTases, for which there is an absolute requirement of divalent magnesium ion for catalysis.[24]

The steady-state kinetics constants for *Mt*HGPRT (**Table 1**) showed an approximately 54-fold larger value for K_m of PRPP as compared to Hx, and 65-fold as compared to Gua. Higher overall K_m values for PRPP compared to Hx or Gua have also been reported for *Homo sapiens* (*Hs*HGPRT) (68-fold for Hx; 18-fold for Gua)[15] and *Plasmodium falciparum* (*Pf*HGPRT) (27-fold for Hx; 53-fold for Gua).[28] *Mt*HGPRT showed a K_m 2.6-fold lower for Gua as compared to Hx. However, the k_{cat}/K_m value was 1.8-fold larger for the HPRT reaction as compared to the GPRT reaction. As k_{cat}/K_m determines the specificity for competing substrates, *Mt*HGPRT appears to be more efficient at using Hx than Gua as co-substrate. Interestingly, *Hs*HGPRT has a k_{cat}/K_m value of 1.3 $x10^7$ for HPRT reaction and 3.7 $x10^6$ for GPRT reaction,[15] indicating a higher efficiency at using both substrates when compared to *Mt*HGPRT. As for *Mt*HGPRT, the apparent second-order rate constant value for *Hs*HGPRT-catalyzed phosphorybosyl transfer to Hx is larger than to Gua.

Double reciprocal patterns of lines intersecting to the left of the *y*-axis (data not shown) are an indication that the reaction catalyzed by *Mt*HGPRT obeys a sequential (either random or ordered) kinetic mechanism, which leads to the formation of a ternary complex capable of undergoing catalysis.[23] Sequential mechanisms have been suggested as one of the features shared by type I PRTases.[24,26,29-31] The pattern of lines intersecting to the left of the y-axis rules out ping-pong (parallel lines), steady-state random (that gives non-linear reciprocal

plots), and rapid-equilibrium ordered (one of the family of lines should cross at a single value on the *y*-axis) mechanisms. However, the double-reciprocal plots alone cannot distinguish between rapid-equilibrium random and steady-state compulsory ordered bi bi mechanisms. Accordingly, ITC studies were performed to help distinguish between these enzyme mechanisms.

Isothermal Titration Calorimetry. ITC measurements were carried out to both determine the order, if any, of addition of substrate to and the order of product release from *Mt*HPRGT enzyme. Formation of *Mt*HGPRT:IMP and *Mt*HGPRT:GMP binary complexes (**Fig. 1 B,C**) were detected by ITC measurements and generated exothermic profiles (heat released to the system). On the other hand, formation of *Mt*HGPRT:PRPP binary complex (**Fig. 1 A**) was characterized by an endothermic profile (heat taken up from the system). No binding of either Hx or PPi to free *Mt*HGPRT was detected (data not shown). Gua could not be tested due to solubility issues, which precluded reliable data collection. ITC data on PRPP, IMP and GMP binding to free *Mt*HGPRT were best fitted to one set of sites binding model, with the *n* values (number of active sites) of 1.81 sites *per* monomer for GMP, 12 for PRPP and fixed as 1 for IMP. This value indicates the number of molecules bound to each enzyme active site with equal affinity. The value of 12 to stoichiometry (*n*) of the PRPP binding to the free *Mt*HGPRT might be related to the instability and purity of the compound (75% according to the supplier).

These ITC results and double-reciprocal plots suggest a sequential compulsory ordered mechanism for *Mt*HGPRT, in which PRPP binds to free enzyme followed by Hx or Gua binding; and PPi is the first product to dissociate followed by the respective monophosphate nucleoside (IMP or GMP) release, leading to the regeneration of free enzyme (**Fig. 6**). A sequential mechanism has been proposed for *Hs*HGPRT,[15] in which PRPP binds first and release of the nucleotide as the last step of the reaction. Sequential mechanisms have also

been suggested for others type I PRTases.[26,32] It should be pointed out that binding of Gua could not be evaluated by ITC studies due to limited solubility in aqueous solutions. Incidentally, attempts were made to measure whether or not Gua binds to free *Mt*HGPRT enzyme using protein fluorescence spectroscopy; however, no reliable data could be obtained due to high inner filter effects (data not shown). Accordingly, here it is assumed that the lack of binding of Hx to free enzyme serves as a surrogate to Gua (no binding to free *Mt*HGPRT), and thus the same kinetic mechanism is followed by both HPRT and GPRT reactions.

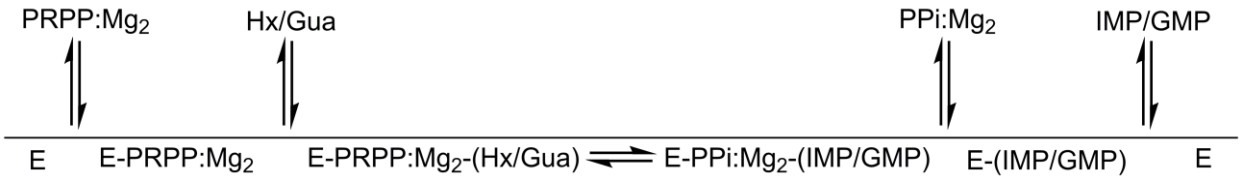

Figure 6. Proposed kinetic enzyme mechanism for *Mt*HGPRT. This order of substrate binding and product release is suggested on basis of the Lineweaver-Burk plots (kinetics) and thermodynamics.

The ITC measurements provided dissociation constants values (K_d) for IMP (130 μM) and GMP (2.1 μM) (**Table 2**). A larger value for IMP as compared to GMP has also been observed for *Hs*HGPRT.[15] The ITC results showed significant heat changes upon ligand (PRPP, IMP, or GMP) binding to free *Mt*HGPRT enzyme (**Fig. 1**), thereby providing thermodynamic signatures of non-covalent interactions to each binding process. Observed enthalpies arise largely as a result of changes in interatomic interactions (e.g., hydrogen bonds and/or van der Waals interactions), in which the sign indicates whether there is a net favourable (negative ΔH) or unfavourable (positive ΔH) redistribution of the network of interactions between the reacting species (including solvent).[33] Hydrophobic interactions are related to the relative degrees of disorder in the free and bound systems and thus these

interactions are reflected in the entropy change. The release of "bound" water molecules from a surface to the bulk solvent is usually a source of favourable entropy (positive ΔS). A reduction in conformational states in either ligand or protein upon binary complex formation is entropically unfavourable (negative ΔS) because this molecular recognition process limits the external rotational and translational freedom of both partners (for instance, structuring regions of the protein adjacent to the bound ligand and loss of conformational freedom of free ligand).[33] The negative ΔH values for IMP and GMP binding (**Table 2**) indicate that these processes are accompanied by favourable redistribution of H-bonds and/or van der Waals interactions. The negative ΔS values for these binding processes are likely coupled to a decrease in conformational states upon binary complex formation. Accordingly, IMP or GMP dissociation from the binary complex to yield free *Mt*HPRT enzyme is likely to be accompanied by an increase in conformational states including the flexible loop involved in binding of nitrogenous base, which is a characteristic feature of type I PRTases.[24] The ITC data also show that GMP binds 68-fold more strongly than IMP, probably due to additional interactions made by the exocyclic amino group of GMP and *Mt*HGPRT.[15] The thermodynamic analysis of binding of PRPP gives a K_d of 48 μM, with favourable entropic contribution and unfavorable binding enthalpy (**Table 2**), indicating that this binding event is accompanied by release of water molecules to bulk solvent and unfavorable redistribution of the hydrogen bond network and/or van der Waals interactions between the reacting species.[33]

The Gibbs free energy values for PRPP, GMP and IMP binding to *Mt*HGPRT (**Table 2**) show that these processes are favourable (negative value for ΔG). As indicated in **Eq. 5**, ΔG consists of enthalpic and entropic contributions, and the results given in **Table 2** are yet additional examples of entropy-enthalpy compensation often observed in biomolecular interactions.[34] If the ligand displays a significant enthalpic contribution, sometimes this contribution is offset by a large entropic compensation, which happens when we compare the

Gibbs free energy of binding of substrate and products to *Mt*HGPRT. For GMP and IMP binding, favorable formation of hydrogen bond and/or van der Waals interactions are accompanied by a likely decrease in conformational states of enzyme and ligand species, thus compensating all gain in the enthalpy. On the other hand, for PRPP the inverse happens: the unfavorable redistribution of the hydrogen bonds is compensated by favorable entropic contribution (e.g., release of "bound" water molecules to solvent), compensating the penalty in enthalpy.[34]

Energy of Activation. The linearity of the Arrhenius plot (**Fig. 3**) suggests that there is no change in the rate-limiting step over the temperature range utilized in the assay for HPRT and GPRT reactions.[20] The E_a values for Hx and Gua, representing the minimum amount of energy necessary to initiate the *Mt*HGPRT-catalyzed chemical reaction, were similar (**Table 3**). The values of free activation energy ($\Delta G^{\#}$) represent the energy barrier required for reactions to occur. The $\Delta G^{\#}$ values can also be regarded as the variation of the Gibbs energy between the activated enzyme:substrate(s) activated complex and enzyme:substrate(s) in the ground state. No differences in $\Delta G^{\#}$ values were observed for the substrates studied here, suggesting a similar overall free activation energy for HPRT and GPRT reactions. The constant A of **Eq. 7** corresponds to the product of collision frequency (Z) and the probability or steric factor (p) from the collision theory of reaction rates. From the absolute rate theory, $A=pZ=(k_BT/h)e^{\Delta S^{\#}/R}$. Accordingly, this equation enables interpretation of the probability factor in terms of entropy of activation. The negative values for the entropy of activation ($\Delta S^{\#}$) for HPRT and GPRT reactions (**Table 3**) suggests that these reactions proceed slower than predicted by the collision theory and that the entropy value for the enzyme:substrate(s) activated complex is lower than the one for enzyme:substrate(s) in the ground state (there is loss of degrees of freedom on going from the ground state to activated state).

Pre-steady State Kinetics. The values for the apparent first-order rate constant for HPRT (0.213 s^{-1}) and GPRT reactions (0.216 s^{-1}) are similar to the catalytic rate constants for Hx (k_{cat} = 0.89 s^{-1}) and Gua (k_{cat} = 0.193 s^{-1}) from steady-state kinetic measurements (**Table 1**). In the study of the transient phase of enzyme reactions, the data obtained are generally expressed by a single exponential curve for the first order reaction.[21] The observation of burst during a time course in the transient phase is an evidence of a significant build-up of product formation along the reaction pathway.[21] If a burst is observed during the transient phase, and the concentration of IMP or GMP produced is approximately equal to the initial *Mt*HGPRT subunit concentration, it would indicate that the chemical step of the reaction is much faster than the release of product (PPi, IMP or GMP). As there is no burst in product formation (**Fig. 2 A, B**), the pre-steady state data demonstrate that product release does not contribute to the rate-limiting step of the chemical reaction catalyzed by *Mt*HGPRT.

Solvent Isotope Effects. Solvent isotope effects were determined to assess whether or not proton transfer from the solvent contributes to the rate of phosphoribosyltransferase reactions catalyzed by *Mt*HGPRT. Isotope effects on V report on events following the ternary complex formation capable of undergoing catalysis (fully loaded enzyme), which include the chemical steps, possible enzyme conformational changes, and product release (leading to regeneration of free enzyme). Solvent isotope effects on V/K report on the contribution of the proton transfer in steps in the reaction mechanism from binding of the isotopically labeled chemical compound (solvent) to the first irreversible step, usually considered to be the release of the first product (that is, all rate constants from reactant binding until the first irreversible step).[35] Accordingly, to evaluate the contribution, if any, of proton transfer from solvent to a rate-limiting step, measurements of solvent isotope effects on V and V/K were carried out. As rule of thumb, deuterium accumulates where binding is tighter (that is, fractionation factor is

larger than one). Transition state proton contributes the reciprocal of its respective fractionation factor to the solvent isotope effect, whereas the contribution of a reactant state proton to the solvent isotope effect is equal to its fractionation factor.[36]

The solvent isotope kinetic effects parameters for HPRT reaction ($^{D2O}V_{PRPP}$, $^{D2O}V/K_{PRPP}$, $^{D2O}V_{Hx}$, $^{D2O}V/K_{Hx}$) suggest modest, if any, participation of the proton solvent in catalysis and binding (**Table 4**). The parameters of GPRT reaction ($^{D2O}V/K_{PRPP}$, $^{D2O}V_{Gua}$, $^{D2O}V/K_{Gua}$) also suggest modest, if any, participation of proton transfer from the solvent in catalysis and binding. On the other hand, the value of 0.71 ± 0.04 suggests an inverse effect on $^{D2O}V_{PRPP}$ (**Table 4**). The expression of deuterium kinetic isotope effect on V includes the intrinsic isotope effect, commitment factors (forward and reverse) and equilibrium isotope effect.[36] The inverse effect on $^{D2O}V_{PRPP}$ suggests that deuterium accumulates (tighter binding) in a transition state from ternary complex to the first irreversible step as transition state protons contribute the reciprocal of its fractionation factor to the kinetic solvent isotope effect (providing equilibrium isotope effect is normal). Solvent isotope effects lead to isotope exchanges at hundreds of protic positions of the enzyme, which precludes any assignment to a particular chemical group. Interestingly, a normal solvent isotope effect for k_{cat} was observed for the HPRT reaction (**Table 4**).

Determination of equilibrium constant. The analysis of the equilibrium experiments for HPRT and GPRT reactions yielded values of 0.0271 for K_{eq} of Hx (**Fig. 4A**) and 0.0357 for K_{eq} of Gua (**Fig. 4B**). The standard free energy ($\Delta G°$) can thus be calculated by **Eq. 13**. This analysis gives values at 25 °C (298.15 K) for $\Delta G°$ of 8.95 kJ mol^{-1} (2.13 kcal mol^{-1}) for Hx and 8.27 kJ mol^{-1} (1.97 kcal mol^{-1}) for Gua. These results suggest that HPRT and GPRT reactions are not favorable processes under at equilibrium. The PRTase reactions display a wide range of K_{eq}, from 0.1 for OPRTase to a value of 300 for APRTase.[15] However, whether

or not phosphoribosyl transfer is a favorable process ($\Delta G < 0$) *in vivo*, the intracellular concentrations of substrates and products need to be determined. There are other MTB enzymes that catalyze reactions that could provide free bases and PRPP. For instance, purine nucleoside phosphorylase (PNP), involved in the metabolism of both purine and pyrimidine.[37] PNP catalyzes the reversible phosphorolysis of the *N*-glycosidic bond of α-purine (deoxy)ribonucleosides to generate ß-(deoxy)ribose 1-phosphate and the corresponding purine bases.[38,39]

pH-rate profile. The pH dependence of kinetic parameters for HPRT and GPRT reactions were carried out to probe acid/base chemistry in *Mt*HGPRT mode of action. The enzyme was stable over the pH range (HPRT reaction: 5.5 - 10; GPRT reaction: 5 - 10) used in pH-rate profiles (data not shown). Multiple sequence alignment of HGPRTs shows the conserved residues involved in catalysis and PRPP binding (**Fig. 7**). The pH dependence of k_{cat} is concerned with the chemical step and its value follows the pK_a of groups that play critical roles in catalysis. The pH-rate data of k_{cat} for HPRT reaction showed a profile of a curve with slope of +1 that goes to zero as a function of increasing pH values (**Fig. 5A**). Fitting the pH-rate data to **Eq.14** yielded a value of 6.3 (± 1.2) for pK_a. In *Hs*HGPRT, Asp137 (Asp123 in *Mt*HGPRT) has been proposed to act as a general acid/base for catalysis and Lys165 (Lys154 in *Mt*HGPRT) as a group involved in ground-state interactions with substrates for nucleotide formation reaction.[40] It is thus tempting to suggest that the residue that needs to be deprotonated for HPRT catalysis to occur can be attributed to the carboxyl side chain of conserved Glu122 or Asp123 of *Mt*HGPRT (**Fig. 7**). Although the pK_a value of the γ-carboxyl group of Glu residues is in the 4.3 – 4.5 range and the β-carboxyl group of Asp residues are usually in the 3.9 – 4.0 range, it is not unlikely that this pK_a value may be displaced by neighbouring chemical groups. Although attempts of fitting the pH-rate data of k_{cat} for GPRT

reaction (**Fig. 5B**) to an equation that describes "hollows" were made,[41] no convergence to any parameters could be achieved. A similar profile was shown for the HPRT reaction catalyzed by *Hs*HGPRT enzyme.[40] Xu and Grubmeyer concluded that this "hollow" possibly arises from slow protonic equilibria for this reaction, in which there are slow proton transfers between enzymatic residues and solvent.[40] The pH dependence of k_{cat}/K_M relates to the required (or preferred) protonation states for binding and/or subsequent catalysis of groups in either the substrate or the enzyme form it combines with.[23] The data for k_{cat}/K_{PRPP} of HPRT and GPRT reactions were fitted to **Eq.14**, yielding values of, respectively, 7.0 (± 0.9) and 6.1 (± 2.8). These data indicate that there is a residue that needs to be deprotonated for productive binding of PRPP. The sequence alignment results show that a highly conserved PRPP binding loop is found in *Mt*HGPRT (**Fig. 7**). This loop starts at Val118 and extends to Leu131, and the presence of two acidic amino acid is believed to be critical for PRPP binding to type I PRTases.[24] As the slopes of k_{cat}/K_{PRPP} for HPRT and GPRT reactions were +1, it seems that either Glu122 or Asp123, which are located in the PRPP binding loop (**Fig. 7**), is the likely group with pK_a values of 7.0 and 6.1 involved in PRPP binding. Interestingly, Xu and Grubmeyer found a bell-shaped profile for k_{cat}/K_{PRPP} data of *Hs*HGPRT for pH values ranging from 5 to 9.5, suggesting Asp137 as the residue with pK_a of 7.1 that needs to be deprotonated and Lys165 as the residue with pK_a of 8.8 that needs to be protonated for productive PRPP binding.[40] The data for k_{cat}/K_{Gua} of GPRT reaction were fitted to **Eq. 14**, yielding a pK_a value of 6.8 (± 2.0). These results suggest that there is a residue that needs to be deprotonated for productive binding of Gua (**Fig. 5B**). At any rate, site-directed mutagenesis should be carried out to provide a solid foundation on the role of amino acids in catalysis and/or substrate binding for *Mt*HGPRT. For the HPRT reaction, no equation could be fitted to the k_{cat}/K_{Hx} data (**Fig. 5A**) and it appears that there is no ionizable group involved in Hx binding in the 5.5 to

10 pH range. Ideally, the crystal structure of *Mt*HGPRT should be determined to provide structural information to help interpretation of the pH-rate data here presented.

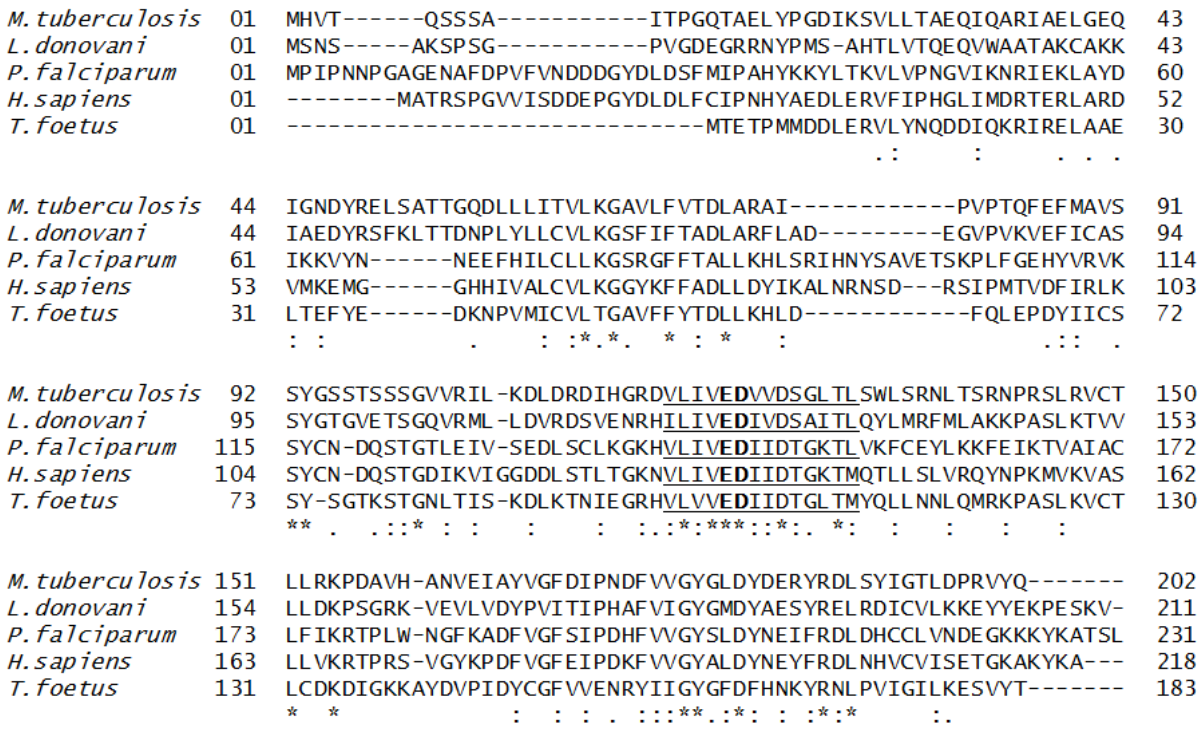

Fig. 7. Multiple sequence alignment of *M. tuberculosis* (UniProt: P9WHQ9), *L. donovani* (UniProt: P43152), *P. falciparum* (UniProt: P20035), *H. sapiens* (UniProt: P00492) and *T. foetus* (UniProt: P51900) HGPRT enzymes. Amino acids for each polypeptide sequence were independently numbered. Identical conserved residues are indicated by stars below the alignment. Multiple sequence alignment was performed with Clustal Omega software (http://www.ebi.ac.uk/Tools/msa/clustalo/). Conserved Aspartic acid 123 (D) and glutamic acid 125 (E) involved in PRPP binding in the PRPP loop (underlined) are highlighted in bold.

Acknowledgments

This work was supported by funds awarded by Decit/SCTIE/MSMCT-CNPq-FNDCT-CAPES to National Institute of Science and Technology on Tuberculosis (INCT-TB) to D.S.S. and L.A.B. L.A.B. and D.S.S. also acknowledge financial support awarded by FAPERGS-CNPq-PRONEX-2009. L.A.B. (CNPq, 520182/99-5), D.S.S. (CNPq, 304051/1975-06) is Research Career Awardee of the National Research Council of Brazil (CNPq). P.C.P. and B.L.A acknowledge scholarships awarded by CAPES. LKBM is a Post-Doctoral Fellow of FAPERGS/CAPES.

References

1. World Health Organization (2014), Global Tuberculosis Report 2013, WHO Press, Geneva.

2. Ducati, R.G., Ruffino-Netto, A., Basso, L.A., and Santos, D.S. (2006) The resumption of consumption- A review on tuberculosis. *Mem. Inst. Oswaldo Cruz* 101 (7), 697-714.

3. Jain A, and Mondal R. (2008) Extensively drug-resistant tuberculosis: current challenges and threats. *FEMS Immunol Med Microbiol* 53, 145–50.

4. Velayati AA, Farnia P, Masjedi MR, Ibrahim TA, Tabarsi P, et al. (2009) Totally drug-resistant tuberculosis strains: evidence of adaptation at the cellular level. *Eur Respir J* 34: 1202–1203.

5. Rustad, T.R., Sherrid A.M., Minch K.J., and Sherman, D. R. (2009) Hypoxia: a window into *Mycobacterium tuberculosis* latency. *Cell. Microbiol*, 11, 1151–1159.

6. Eisenreich, W., Dandekar T., Heesemann J., and Goebel, W. (2010) Carbon metabolism of intracellular bacterial pathogens and possible links to virulence. *Nat. Rev. Microbiol.* 8, 401–412.

7. Niederweis, M., (2008) Nutrient acquisition by mycobacteria. *Microbiology* 154, 679–692.

8. Kantardjieff, K.A., Vasquez, C., Castro, P., Warfel, N.M., Rho, B.S., Lekin, T., Kim, C.Y., Segelke B.W., Terwilliger, T.C., and Rupp, B. (2004) Structure of *pyrR* (Rv1379) from *Mycobacterium tuberculosis*: a persistence gene and protein drug target. *Acta Crystallogr., D* 61, 355–364.

9. Parker, W.B., and Long, M.C. (2007) Purine metabolism in *Mycobacterium tuberculosis* as a target for drug development. *Curr. Pharm. Des*. 13 599–608.

10. Munagala, N., Basus, V.J., and Wang C.C. (2001) Role of the flexible loop of hypoxanthine-guanine-xanthine phosphoribosyltransferase from *Tritrichomonas foetus* in enzyme catalysis. *Biochemistry* 40, 4303-4311.

11. Musick, D.L. (1981) Structural features of the phosphorybosil-transferases and their relationship to the human deficiency disorders of purine and pyrimidine metabolism. *CRC Crit. Rev. in Biochem.*11, 1-34.

12. Eads, J.C., Scapin, G., Xu, Y., Grubmeyer, C., and Sacchettini, J.C. (1994) The crystal structure of human hypoxanthine-guanine phosphoribosyltransferase with bound GMP. *Cell* 78, 325-334.

13. Munagala, N. R., Chin, M. S., and Wang, C. C. (1998) Steady-state kinetics of the hypoxanthine-guanine-xanthine phosphoribosyltransferase from *Tritrichomonas foetus*: the role of threonine-47. *Biochemistry* 37, 4045-4051.

14. Page, J. P., Munagala, N. R., and Wang, C. C. (2001) Point mutations in the guanine phosphoribosyltransferase from *Giardia lamblia* modulate pyrophosphate binding and enzyme catalysis. *Eur. J.Biochem*. 259, 565-571.

15. Xu, Y., Eads, J., Sacchettini, J.C., and Grubmeyer, C. (1997) Kinetic mechanism of human hypoxanthine-guanine phosphoribosyltransferase: rapid phosphoribosyl transfer chemistry. *Biochemistry* 36, 3700-3712.

16. Yuan, L., Craig, S. P. 3rd., McKerrow, J. H., and Wang, C. C. (1992) Steady-state kinetics of the schistosomal hypoxanthine-guanine phosphoribosyltransferase. *Biochemistry* 31, 806-810.

17. Torres R.J., and Puig J.G. (2007) Hypoxanthine–guanine phosphoribosyltransferase (HPRT) deficiency: Lesch–Nyhan syndrome, Orphanet *J. Rare Dis*. 2 48.

18. Wenck M.A., Medrano F.J., Eakin A.E., and Craig S.P. (2004) Steady-state kinetics of the hypoxanthine phosphoribosyltransferase from *Trypanosoma cruzi*. *Biochim. Biophys. Acta.* 1700, 11–18.

19. Biazus, G., Schneider, C.Z., Palma, S.M., Basso, L.A., and Santos, D.S. (2009) Hypoxanthine-guanine phosphorybosiltransferase from *Mycobacterium tuberculosis* H37Rv: Cloning, expression, and biochemical characterization. *Prot. Exp. and Pur*. 66, 185-190

20. Segel, I.H. (1975) Enzyme kinetics, behavior and analysis of rapid equilibrium and steady-state enzyme systems. New York, John Wiley and Sons, Inc.

21. Hiromi. K. (1979) Kinetics of Fast Enzyme Reactions: Theory and Practice, Kodansha Ltd., Tokyo, chapter. 4, pp. 188–253.

22. Lonhienne, T., Baise E., Feller G., Bouriotis V., and Gerday C. (2001) Enzyme activity determination on macromolecular substrates by isothermal titration calorimetry: application to mesophilic and psychrophilic chitinases. *Biochim. Biophys. Acta* 1545, 349–356.

23. Cook P.F., and Cleland, W.W. (2007) Enzyme Kinetics and Mechanism, Garland Science Publishing, New York, pp. 253–323.

24. Sinha, S.C., and Smith, J.L. (2001) The PRTase protein family. *Curr. Opin. Struct. Biol*. 11, 733–739.

25. Victor, J., Leo-Mensah, A., and Sloan, D.L. (1979) Divalent metal ion activation of the yeast orotate phosphoribosyltransferase catalyzed reaction. *Biochemistry* 18, 3597–3604.

26. Breda, A., Rosado, L.A., Lorenzini, D.M., Basso, L.A., and Santos, D.S. (2012) Molecular, kinetic and thermodynamic characterization of *Mycobacterium tuberculosis* orotate phosphoribosyltransferase. *Mol. BioSyst*. 8, 572–586

27. Salerno, C., and Giacomello, A. (1981) Human hypoxanthine guanine phosphoribosyltransferase: The role of magnesion ion in a phosphorybosylpyrophosphate-utilizing enzyme. *J. Bio. Chem.* 256, 3671-3673.

28. Subbayya, I.N.S., and Balaran, H. (2002) A point mutation at the subunit interface of hypoxanthine-guanine-xanthine phosphoribosyltransferase impairs activity: role of oligomerization in catalysis. *FEBS Letters* 521, 72-76.

29. Krungkrai S. R., Aoki, S., Palacpac, N.M.Q., Sato, D., Mitamura, T., Krungkrai J., and Horii T. (2004), Human malaria parasite orotate phosphoribosyltransferase: functional expression, characterization of kinetic reaction mechanism and inhibition profile. *Mol. Biochem. Parasitol*. 134, 245–255.

30. Wang, G.P., Lundegaard, C., Jensen, K.F., and Grubmeyer C. (1999) Kinetic mechanism of OMP synthase: a slow physical step following group transfer limits catalytic rate. *Biochemistry* 38, 275–283.

31. Villela, A.D., Ducati, R.G., Rosado, L.A., Bloch, C.J., Prates, M.V., Gonçalves, D.C., Ramos, C.H.I., Basso, L.A., and Santos, D.S. (2013). Biochemical characterization of uracil phosphoribosyltransferase from *Mycobacterium tuberculosis*. *Plos One* 8.

32. Kwong P., Doyle, M.L., Casper, D.J., Cicala, C., Leavitt S.A., Majeed, S., Steenbeke T.D., Venturi, M., Chaiken, I., Fung M., Katinger H., Parren, P.W., Robinson, J., Van Ryk, D., Wang, L., Burton, D.R., Freire E., Wyatt R., Sodroski J., Hendrickson, W.A., and Arthos J. (2002) HIV-1 evades antibody-mediated neutralization through conformational masking of receptor-binding sites. *Nature* 420, 678–682.

33. Ladbury J.E., and Doyle M.L. (2004) Biocalorimetry II. London, Wiley.

34. Chodera, D.J., and Mobley, L.D. (2013) Entropy-enthalpy compensation: ramifications in biomolecular ligand recognition and design. *Annu. Rev. Biophys.* 42, 121-142.

35. Northrop, D.B. (1975) Steady-state analysis of kinetic isotope effects in enzymic reactions. *Biochemistry* 14, 2644–2651.

36. Cook P.F. (1991) Enzyme Mechanism from Isotope Effects. CRC Press, Boca Raton, pp. 203–228.

37. Mascia L., Cappiello M., Cherri S., Ipata P.L. (2000) In vitro recycling of alpha-D-ribose 1-phosphate for the salvage of purine bases. *Biochim. Biophys. Acta* 1474.

38. Kalckar H.M. (1947) Differential spectrophotometry of purine compounds by means of specific enzymes; determination of hydroxypurine compounds. *J. Biol. Chem*. 167 429–443.

39. Porter D.J. (1992) Purine nucleoside phosphorylase. Kinetic mechanism of the enzyme from calf spleen. *J. Biol. Chem.* 267 7342–7351.

40. Xu, Y., and Grubmeyer, C. (1998) Catalysis in human hypoxanthine-guanine phosphorybosiltransferase: Asp 137 acts as a general acid/base. *Biochemistry* 37, 4114-4124.

41. Cook P.F., and Cleland, W.W. (2007) Enzyme Kinetics and Mechanism, Garland Science Publishing, New York, pp. 325–366.

CAPÍTULO 3

DISCUSSÃO GERAL

Para o estudo do modo de ação da HGPRT de *Mycobacterium tuberculosis* foram realizados diversos experimentos: O primeiro deles, apresentado no Capitulo 2, tinha como objetivo a determinação do estado oligomérico em solução da *Mt*HGPRT. A cromatografia de exclusão por tamanho resultou em um valor de 46 kDa, indicando que a enzima se comporta como um dímero em solução. Este resultado está de acordo com a literatura, uma vez que as PRTases tipo 1 são, predominantemente, homodímeros.[32] O seguinte experimento visava a determinação das constantes cinéticas verdadeiras. Primeiramente, executamos testes de atividade sem adição de Mg^{2+}. Como atividade enzimática não foi observada na ausência de Mg^{2+}, podemos inferir que Mg_2:PRPP é o verdadeiro substrato para *Mt*HGPRT, visto que a literatura apresenta que ions divalentes são essenciais para reações catalisadas por PRTases, ativando o substrato PRPP. [33.34] As constantes cinéticas obtidas em estado estacionário, quando foram comparadas com as apresentadas na literatura.[30] As constantes de Michaelis (K_m) obtidas para PRPP quando comparadas com Hx ou Gua se mostraram mais de 50 vezes maiores. Estes valores mais altos também foram observados para *Plasmodium falciparum e Homo sapiens*. [35,36] A *Mt*HGPRT demonstrou um valor de Km 2,6 vezes mais baixo para Gua quando comparado com Hx. No entanto, o valor de k_{cat}/K_m para a reação de HPRT é 1,8 vezes maior quando comparado com a GPRT. Isso deve se dar devido ao valor de k_{cat} maior para HPRT quando comparado com GPRT. Na HGPRT humana o valor de k_{cat}/K_m para ambas as reações é muito mais alto que na *Mt*HGPRT, indicando uma maior eficiência. O gráfico de Lineweaver-Burk (Figura 6) revelou um padrão de retas se encontrando à esquerda do eixo *y*, um indicativo de mecanismo cinético sequencial (podendo ser ordenado ou aleatório), que leva a formação de um complexo ternário, capaz de sofrer catálise. Este mecanismo é sugerido como uma característica das PRTases tipo 1. [32,37]

Figura 6. Gráficos de Lineweaver-Burk.

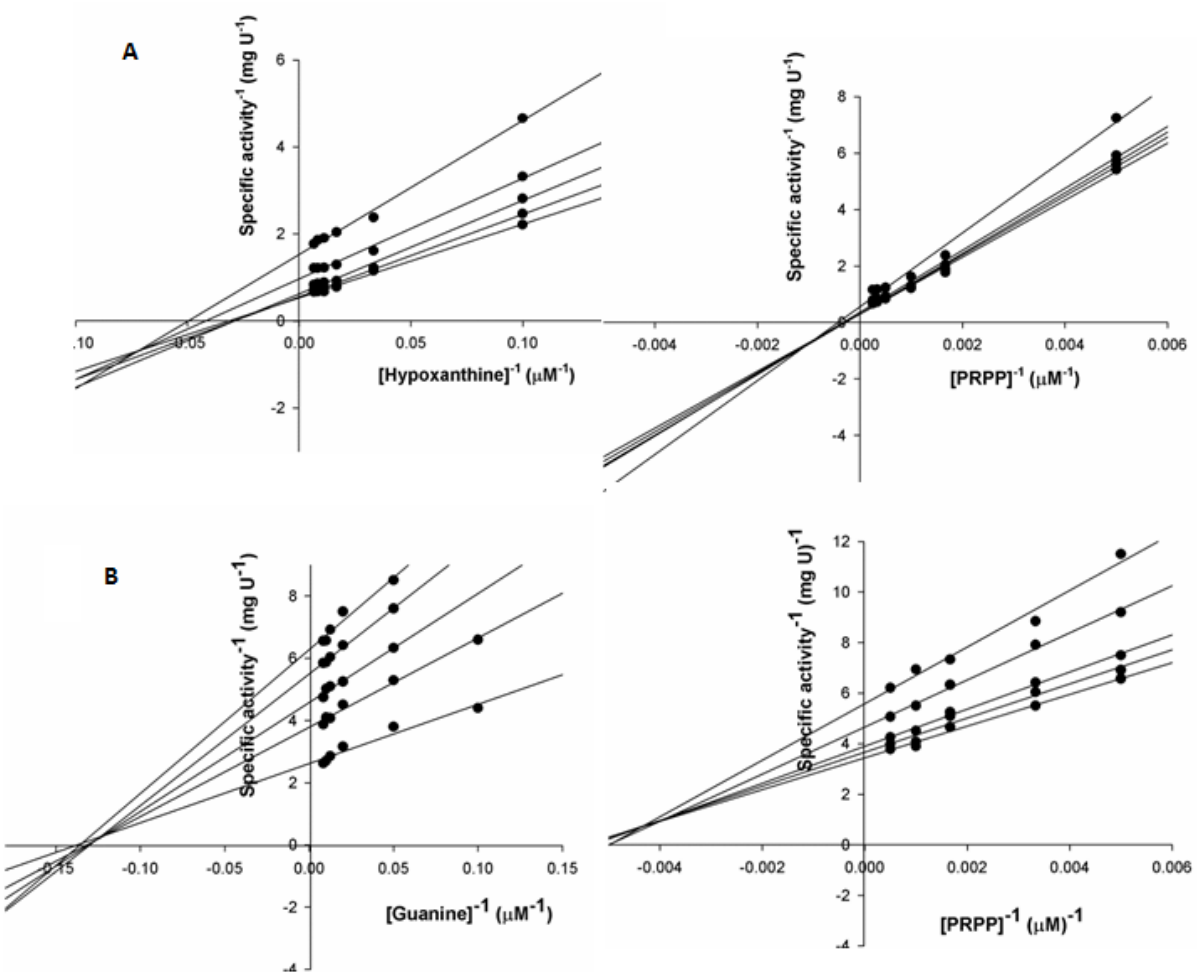

Fonte: Autor.
Nota: O padrão de retas nos gráficos de Lineweaver-Burk indica o possível mecanismo cinético da enzima. O padrão de retas se encontrando a esquerda do eixo *y* indica um mecanismo cinético sequencial, ordenado ou aleatório. Este padrão pode ser observado para ambos os substratos nas reações de HPRT (A) e GPRT (B).

Para a determinação da ordem, se existente, foram realizados experimentos em microcalorímetro. Estes experimentos demonstraram a formação de complexos binários de PRPP, IMP e GMP com *Mt*HGPRT. Não foi observada a ligação de Hx ou PPi na enzima livre. Devido a problemas de solubilidade não foi possível o teste utilizando Gua. Estes resultados corroboram o mecanismo cinético sequencial ordenado, onde PRPP liga-se na enzima, seguido da base livre (Hx ou Gua) e, após a catálise ocorre a liberação de PPi e o nucleosídeo monofosfato (IMP ou GMP). [37] A figura 7 ilustra a sequência sugerida de adição e liberação.

Figura 7. Mecanismo cinético proposto para a enzima MtHGPRT.

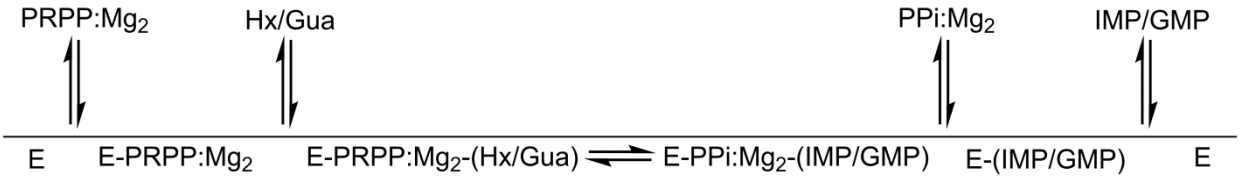

Os experimentos em ITC também proveram os valores de dissociação (*K*d) para IMP (133.8 µM) e GMP (2.1 µM) Este valor mais baixo para o GMP em relação ao IMP também é observado na HGPRT humana.[36] A maior afinidade pelo GMP pode ser explicada pela ligação de hidrogênio extra realizada pela molécula.[36]

Os experimentos de energia de ativação (E_a) foram realizados para identificação de efeitos da temperatura na catálise, bem como extração das constantes termodinâmicas no estado de transição. O gráfico de Arrhenius demonstrou que a temperatura não influencia na etapa limitante. Os valores de E_a para Hx e Gua foram similares, representando a mínima energia necessária para iniciar a reação química da *Mt*HGPRT.

Os estudos de cinética em estado pré-estacionário foram conduzidos para a identificação de um possível efeito de "burst", onde a possível etapa limitante seria a liberação dos produtos e duas velocidades seriam observada, porém este efeito não foi observado. Os valores para constante de primeira ordem obtidos foram comparados com o k_{cat} foram similares.

Para os estudos da contribuição da transferência de próton, foram realizados experimentos de velocidade inicial em espectrofotômetro. Os valores de *V* indicam eventos relacionados com a formação do complexo ternário capaz de sofrer catálise, incluindo as possíveis alterações conformacionais, etapas químicas e liberação dos produtos. Efeitos em *V/K* reportam a contribuição da transferência de próton na ligação dos substratos até a primeira etapa irreversível, geralmente considerada a liberação do primeiro produto. Os resultados apresentados no capítulo 2 para este experimento demonstraram que não há efeito isotópico, ou seja, não há contribuição da transferência do próton na etapa limitante.

Para a determinação da constante de equilíbrio (K_{eq}) da *Mt*HGPRT para ambas as reações, foram realizados experimento em espectrofotômetro, onde uma razão nas concentrações de base (Hx ou Gua) e nucleosídeo monofosfato (IMP ou GMP) foi mantida fixa em 1 enquanto a razão entre PPi e PRPP foi variada. Este experimento resultou nos valores de 0,0217 para

Hx e 0,0357 para Gua. Isto indica que ambas as reações não são espontâneas. Porém, é necessário se saber as concentrações intracelulares de substratos e produtos para se determinar qual reação (*forward* ou *reverse*) acontece. É importante relembrar que existem outras enzimas que são capazes de prover as bases para as reações, como é o caso da purina nucleosídeo fosforilase (PNP), envolvida no metabolismo de purinas e pirimidinas. [38]

Por fim, para o estudo do efeito do pH sobre dos parâmetros cinéticos para ambas as reações catalisadas pela *Mt*HGPRT o perfil de pH foi realizado. Primeiramente a estabilidade da enzima foi testada em diversos pHs. O efeito do pH sobre k_{cat} está relacionado com a etapa química e os valores relacionados com o p*K* de cadeias laterais de aminoácidos que possuem papeis relevantes na catálise. O valor para o pK_a obtido para k_{cat} para a reação de HPRT foi 6,3. Na HGPRT humana Asp 137 faz parte da catálise ácido/base junto com a lisina 165 (154 em *Mt*HGPRT), sendo responsável pela desprotonação e protonação do N7 do anel purínico. [39] Nenhuma equação pode ser aplicada para o plot de k_{cat} para a reação de GPRT, indicando que, nos pHs testados, não houve alteração desta constante de primeira ordem. Em relação a dependência do k_{cat}/K_M com o pH, que está relacionada com a etapa de ligação do substrato com a enzima, o valor para PRPP para ambas as reações foi obtido através da mesma equação utilizada anteriormente. Os valores foram de 7 e 6,1 respectivamente. De acordo com o alinhamento (figura 8) e com a literatura,[32] uma alça de ligação de PRPP altamente conservado pode ser encontrado em *Mt*HGPRT. Este loop começa na Val 118 e se extende até a Leu 131, e a presença de dois aminácidos ácidos aparentemente é crítica para todas as PRTases tipo 1 para que haja a ligação do PRPP.[32] É possível, então, atribuir o valor de p*K*a 7 e 6,1 para Glu 122 ou Asp 123, uma vez que a cadeia lateral ácida de ambos os aminoácidos podem formar ligações de hidrogênio com os grupamentos hidroxila da ribose do PRPP.

Não é possível afirmar, no entanto, se ambos ou apenas um dos aminoácidos são necessários para a ligação do PRPP. Uma forma de se estudar este evento seria a aplicação de mutagênese sítio-dirigida, onde estes aminoácidos poderiam ser substituídos por outros, com diferentes cadeias laterais, permitindo o entendimento do papel destes aminoácidos.

Para a reação de GPRT a mesma equação foi utilizada para a dependência do pH no $k_{cat}/K_{Gua,}$ resultando no valor de 6,8. O alinhamento (Figura 8) mostra a presença de uma lisina

conservada que pode interagir com o substrato Gua. Na HGPRT humana esta lisina (Lys165) interage, através de ligação de hidrogênio com o grupamento cabonila do GMP.[36]

Figura 8. Alinhamento múltiplo.

Nota: Alinhamento multiplo de HGPRT de *M. tuberculosis* (UniProt: P9WHQ9), *L. donovani* (UniProt: P43152), *P. falciparum* (UniProt: P20035), *H. sapiens* (UniProt: P00492) and *T. foetus* (UniProt: P51900) realizado no software Clustal Omega (http://www.ebi.ac.uk/Tools/msa/clustalo/). Os aminoácidos destacados em negrito são conservados e apresentam papel relevante na ligação ou catálise. Alça de ligação ao PRPP foi sublinhado para destaque.

CAPÍTULO 4

CONSIDERAÇÕES FINAIS

A HGPRT desempenha um papel importante na via de salvamento de MTB, participando na reciclagem de bases purínicas. Esta via necessita de menos energia, uma vez que a via de salvamento necessita de onze reações para a obtenção dos mesmos produtos. O estudo do modo de ação da HGPRT permite a compreensão de como a enzima se comporta, quais suas propriedades cinéticas, a ordem de adição de substratos e liberação de produtos (mecanismo cinético) e o efeito do pH em resíduos relevantes para a ligação e/ou catálise. Este estudo foi feito através de cinética em estado estacionário, onde foram obtidas as constantes cinéticas verdadeiras para os substratos, influência da temperatura, efeitos isotópicos e do pH na reação catalisada pela enzima. Estudos em ITC também foram realizados, corroborando o mecanismo proposto pela cinética e determinando a ordem de adição dos substratos/produtos. Estes experimentos também permitiram a obtenção dos valores de dissociação (K_d), a estequiometria da reação e contribuições entálpicas e entrópicas, bem como a energia livre de Gibbs da ligação. A determinação da estrutura tridimensional da *Mt*HGPRT em sua forma livre ou complexada com um substrato, produto ou análogo poderia indicar as diferenças estruturais quando comparada com as HGPRTs de outros organismos, e também relacionadas com as diferenças entre as constantes obtidas.

Nós esperamos que os resultados obtidos neste trabalho contribuam para o entendimento do modo de ação da HGPRT na via de salvamento de purinas de *Mycobacterium tuberculosis*, uma vez que este patógeno ainda é uma ameaça global e que requer atenção da comunidade científica. No entanto, alguns estudos ainda devem ser realizados para a melhor compreensão do modo de ação da enzima, como por exemplo o *knockout* do gene e mutagênese sitio-dirigidas, o que corroboraria os aminoácidos importantes para o funcionamento da *Mt*HGPRT.

REFERÊNCIAS

1. Lawn SD, Zumla AI. Tuberculosis. **The Lancet.** 2011; 378:57-72.

2. Ducati RG, Ruffino-Neto A, Basso LA, Santos DS. The resumption of consumption – A review on tuberculosis. **Ment Inst Oswaldo Cruz.** 2006; 101: 697-714.

3. Smith NH, Hewinson RG, Kremer K, Brosch R, Gordon SV. Myths and misconceptions: the origin and evolution of *Mycobacterium tuberculosis*. **Nat. Rev. Microbiol.** 2009; 537-540.

4. Bloom BR, Murray CJL. Tuberculosis: commentary on a reemergent killer. **Science.** 1992; 257:1055-64.

5. Gengenbacher M, Kaufmann SH. *Mycobacterium tuberculosis*: success through dormancy. **FEMS Microbiol Rev**. 2012 514-32.

6. Palomino JC, Leão SC, Ritacco V. Tuberculosis 2007 - From basic science to patient care. Disponível em: <http://www.freebooks4doctors.com/pdf/tuberculosis2007.pdf>. Acesso em: janeiro de 2013.

7. Jarlier V, Nikaido H. Mycobacterial cell wall: Structure and role in natural resistance to antibiotics. **FEMS Microbiol Lett**. 1994;123:11-18.

8. Disponível em <http://www.who.int/mediacentre/factsheets/fs104/en/index.html>. Acesso em junho de 2014.

9. Zumla AI, Raviglione M, Hafner R, von Reyn CF. Tuberculosis. **N Engl J Med**. 2013 Fev 21 (8): doi: 10.1056

10. Epidemiológica. Manual de recomendações para o controle da tuberculose no Brasil / Ministério da Saúde, Secretaria de Vigilância em Saúde, Departamento de Vigilância Epidemiológica. Brasília: Ministério da Saúde. 2011;284.

11. Flynn JL, Chan J. Immunology of tuberculosis. **Annu Rev Immunol.** 2001;19:93-129.

12. Elston JWT, Thaker HKB. Co-infection with human immunodeficiency virus and tuberculosis. **Indian J Dermatol Venereol Leprol.** 2008;74:194-198.

13. Koul A, Arnoult E, Lounis N, Guillemont J, Andries K. The challenge of new drug discovery for tuberculosis. **Nature**. 2011; 483-90.

14. Russel DG. Who puts the tubercle in tuberculosis? **Nat Rev Microbiol**. 2007; 5:39 47.

15. Lamichhane G. Novel targets in *M. tuberculosis*: search for new drugs**. Trends in molecular medicine.** 2011; 17: 25-33.

16. Yew WW, Leung CC. Management of multidrug-resistant tuberculosis: Update 2007. **Respirology.** 2008;13:21-46.

17. Jassal M, Bishai WR. Extensively drug-resistant tuberculosis. **Lancet Infect Dis**. 2008. Epub 2008 Nov 5.

18. Centers for Disease Control and Prevention. Emergence of Mycobacterium tuberculosis with extensive resistance to second-line drugs - worldwide, 2000-2004. **MMWR Morb Mortal Wkly Rep**. 2006;55:301-305.

19. Cole ST, Brosch R, Parkhill J, Garnier T, Churcher C, Harris D, et al. Deciphering the biology of *Mycobacterium tuberculosis* from the complete genome sequence. **Nature.** 1998; 393(6685):537-44.

20. Parker WB, Long MC. Purine metabolism in *Mycobacterium tuberculosis* as a target for drug development. **Curr Phar Des.** 2007; 13(6):599-608.

21. Ducati RG, Breda A, Basso LA, Santos DS. Purine salvage pathway in mycobacterium tuberculosis. **Curr Med Chem**. 2011;1258-75.

23. Voet D, Voet JG. Bioquímica. 3a ed. Porto Alegre: Artmed Editora S.A.; 2006.

24. Craig SP, Eakin AE. Purine Phosphoribosyltransferases. **Journal of Biol Chem**. 2000;275(27):20231-4.

25. Musick DL. Structural features of the phosphorybosil-transferases and their relationship to the human deficiency disorders of purine and pyrimidine metabolism. **CRC Crit. Rev**. **in Biochem**.1981 11, 1-34.

26. Eads JC, Scapin G, Xu Y, Grubmeyer C, Sachettini JC. The crystal structure of human hypoxanthine-guanine phosphoribosyltransferase with bound GMP. **Cell** 1994. 78, 325-334.

27. Munagala NR, Chin MS, Wang CC. Steady-state kinetics of the hypoxanthine-guanine-xanthine phosphoribosyltransferase from *Tritrichomonas foetus*: the role of threonine-47. **Biochemistry** 1998; 37, 4045-4051.

28. Yuan L, Craig SP3rd, McKerrow JH, Wang CC. Steady-state kinetics of the schistosomal hypoxanthine-guanine phosphoribosyltransferase. **Biochemistry.** 1992; 31, 806-810.

29. Munagala N, Basus VJ, Wang CC. Role of the flexible loop of hypoxanthine-guanine-xanthine phosphoribosyltransferase from *Tritrichomonas foetus* in Enzyme Catalysis. **Biochemistry** 2001; 40, 4303-4311.

30. Xu Y, Eads J, Sacchettini JC, Grubmeyer C. Kinetic mechanism of human hypoxanthine-guanine phosphoribosyltransferase: rapid phosphoribosyl transfer chemistry. **Biochemistry**. 1997;(36) 3700-3712.

31. Biazus G, Schneider CZ, Palma MS, Basso LA, Santos DS. hypoxantine-guanine phosforibosyltransferase from *Mycobaterium tuberculosis* H37Rv: Cloning, expression, and biochemical characterization. **Prot. Exp. and Pur**. 2009;66(2):185-90.

32. Sinha SC, Smith JL. The PRTase protein family. **Curr. Opin. Struct. Biol**. 2001; 11, 733–739.

33. Victor J, Leo-Mensah A, Sloan DL. Divalent metal ion activation of the yeast orotate phosphoribosyltransferase catalyzed reaction. **Biochemistry**, 1979; 18, 3597–3604.

34. Salerno, C., Giacomello, A., Human hypoxanthine guanine phosphorybosiltransferase: The role of magnesium ion in a phosphorybosylpyrophosphate-utilizing enzyme. **J. Bio. Chem**. 1981; 256, 3671-3673.

35. Subbayya INS, Balaran H. A point mutation at the subunit interface of hypoxanthine-guanine-xanthine phosphorybosiltransferase impairs activity: role of oligomerization in catalysis. **FEBS Letters**, 2002; 521, 72-76.

36. Xu Y, Eads J, Sacchettini JC, Grubmeyer C. Kinetic Mechanism of Human Hypoxanthine-Guanine Phosphoribosyltransferase: Rapid Phosphoribosyl Transfer Chemistry. 1997 **Biochemistry** 36, 3700-3712.

37. Breda A, Rosado LA, Lorenzini DM, Basso LA, Santos DS. Molecular, kinetic and thermodynamic characterization of *Mycobacterium tuberculosis* orotate phosphoribosyltransferase. **Mol. BioSyst**. 2012; 8, 572–586

38. L. Mascia, M. Cappiello, S. Cherri, P.L. Ipata.*In vitro* recycling of alpha-D-ribose 1-phosphate for the salvage of purine bases. **Biochim. Biophys. Acta**. 2000; 1474.

39. Xu Y, Grubmeyer C. Catalysis in human hypoxanthine-guanine phosphorybosiltransferase: Asp 137 acts as a general acid/base. **Biochemistry.** 1998; 37, 4114-4124.

Anexo A

Biochemistry - Manuscript ID bi-2014-00979m

onbehalfof+support+services.acs.org@manuscriptcentral.com on behalf of support@services.acs.org
Sent: Wednesday, August 06, 2014 12:49 PM
To: Luiz Augusto Basso

06-Aug-2014

Dear Dr. Basso:

Your manuscript has been successfully submitted to Biochemistry.
Title: "Mode of Action of Recombinant Hypoxanthine-Guanine Phosphoribosyltransferase from Mycobacterium tuberculosis"
Authors: Patta, Paulo; Martinelli, Leonardo; Abbadi, Bruno; Santos, Diogenes; Basso, Luiz
Manuscript ID: bi-2014-00979m.

Please reference the above manuscript ID in all future correspondence or when calling the office for questions. If there are any changes in your contact information, please log in to ACS Paragon Plus at https://acs.manuscriptcentral.com/acs and select "Edit Your Account" to update that information.

You can view the status of your manuscript by checking your "Authoring Activity" tab on ACS Paragon Plus after logging in to https://acs.manuscriptcentral.com/acs.

Thank you for submitting your manuscript to Biochemistry.

Sincerely,

Biochemistry Editorial Office